AD-A058 693 ARNOLD ENGINEERING DEVELOPMENT CENTER ARNOLD AIR FORC--ETC F/G 20/13
HEAT-TRANSFER TESTS ON THE NOSE OF THE SHUTTLE ORBITER EXTERNAL--ETC(U)
JUN 78 D B CARVER, D E BOYLAN

UNCLASSIFIED AEDC-TSR-78-V11 NL

1 OF 1
AD A058 693

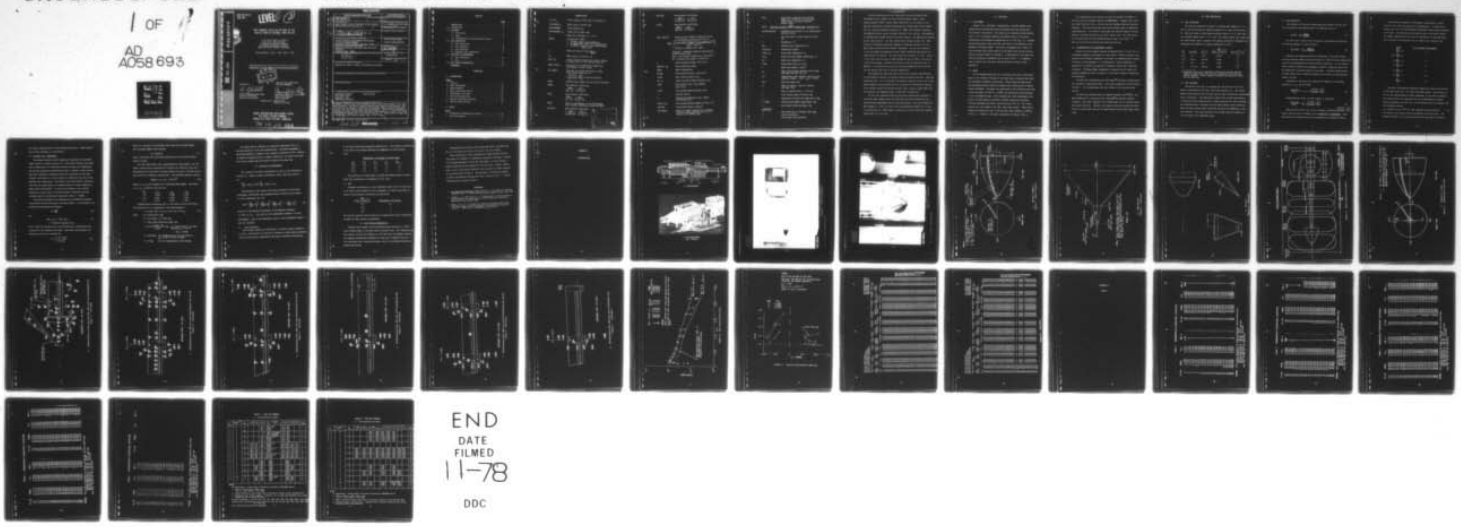

END
DATE FILMED
11-78
DDC

AEDC-TSR-78-V11
JUNE 1978

LEVEL II (2)

HEAT TRANSFER TESTS ON THE NOSE OF THE SHUTTLE ORBITER EXTERNAL TANK (FH-15)

D. B. Carver and D. E. Boylan
ARO, Inc., AEDC Division
A Sverdrup Corporation Company
von Kármán Gas Dynamics Facility
Arnold Air Force Station, Tennessee

Period Covered: May 1, 1978 - May 5, 1978

Approved for public release; distribution unlimited.

Reviewed by:

Ervin P. Jaskolski

ERVIN P. JASKOLSKI, Captain, USAF
Test Director, VKF Division
Directorate of Test Operations

Approved for Publication:
FOR THE COMMANDER

Chauncey D. Smith, Jr.

CHAUNCEY D. SMITH, JR, Lt Colonel, USAF
Director of Test Operations
Deputy for Operations

Prepared for: NASA-JSC/ES3
Houston, TX 77058

ARNOLD ENGINEERING DEVELOPMENT CENTER
AIR FORCE SYSTEMS COMMAND
ARNOLD AIR FORCE STATION, TENNESSEE

UNCLASSIFIED

REPORT DOCUMENTATION PAGE		READ INSTRUCTIONS BEFORE COMPLETING FORM
1. REPORT NUMBER (14) AEDC-TSR-78-V11	2. GOVT ACCESSION NO.	3. RECIPIENT'S CATALOG NUMBER (9)
4. TITLE (and Subtitle) (6) Heat-Transfer Tests on the Nose of the Shuttle Orbiter External Tank (FH-15).		5. TYPE OF REPORT & PERIOD COVERED (12) Final Report, May 1-5, 1978
		6. PERFORMING ORG. REPORT NUMBER
7. AUTHOR(s) (10) D. B. Carver and D. E. Boylan, ARO, Inc., a Sverdrup Corporation Company		8. CONTRACT OR GRANT NUMBER(s)
9. PERFORMING ORGANIZATION NAME AND ADDRESS Arnold Engineering Development Center/DOOV Air Force Systems Command Arnold Air Force Station, Tennessee 37389		10. PROGRAM ELEMENT, PROJECT, TASK AREA & WORK UNIT NUMBERS Program Element 921E01
11. CONTROLLING OFFICE NAME AND ADDRESS National Aeronautics and Space Administration (JSC/ES3) Houston, Texas 77058		12. REPORT DATE (11) June 1978
		13. NUMBER OF PAGES 42
14. MONITORING AGENCY NAME & ADDRESS (if different from Controlling Office) (12) 44p.		15. SECURITY CLASS. (of this report) UNCLASSIFIED
		15a. DECLASSIFICATION/DOWNGRADING SCHEDULE N/A

16. DISTRIBUTION STATEMENT (of this Report)

Approved for public release; distribution unlimited.

17. DISTRIBUTION STATEMENT (of the abstract entered in Block 20, if different from Report)

18. SUPPLEMENTARY NOTES

19. KEY WORDS (Continue on reverse side if necessary and identify by block number)

aerodynamic heating
wind tunnel tests
supersonic flow
interference heating
space shuttle

20. ABSTRACT (Continue on reverse side if necessary and identify by block number)

Aerodynamic heating tests were conducted using a 0.0275-scale model of the space shuttle external tank nose to obtain detailed heat-transfer distributions. Special emphasis was placed on evaluating interference heating around the forward fairing, trays and gaseous oxygen line and brackets. The thin-skin thermocouple technique was used, and data were obtained at Mach numbers 3, 4, and 5.5 at free-stream Reynolds numbers of 3.7 and 5.0 million per ft. Model angle of attack was 0, and ±5 deg, with sideslip angles from -11 to +11 deg.

(+ or −)

DD FORM 1 JAN 73 1473 EDITION OF 1 NOV 65 IS OBSOLETE

042550 UNCLASSIFIED 08 034 4B

CONTENTS

APPENDIXES

A. ILLUSTRATIONS

B. TABLES

NOMENCLATURE

a_1, a_2, a_3	Denote constant terms used to calculate R
ALPHA-MODEL, α	Model angle of attack, deg
ALPHA-PREBEND	Sting prebend, deg
ALPHA-SECTOR, α_s	Tunnel sector angle, deg
b	Model wall thickness, in., or ft
CONFIG	Configuration number 1. ET NOSE - Model with hardware on 2. ET NOSE/CLEAN - Model with hardware off 3. ET NOSE/T - Same as 1 but using boundary layer trips
c_p	Model wall specific heat, $\frac{\text{Btu}}{\text{lbm-°R}}$
CR	Model center of rotation, in.
DELY, ΔY	Lateral distance along an arc sector relative to cable tray, θ = 31.5 deg (see Fig. 5b)
DTWDT, dTW/dt	Derivative of the model wall temperature with respect to time, °R/sec
FIT LENGTH	Time span in seconds over which a linear least-squares curve fit of $\ell n \left[\frac{0.95\ TO - TW_i}{0.95\ TO - TW}\right]$ vs time was applied
GROUP	Identification number for each tunnel injection
H(TAW)	Heat-transfer coefficient, $\frac{QDOT}{TAW - TW}, \frac{\text{Btu}}{\text{ft}^2\text{-sec-°R}}$
H(TO)	Heat-transfer coefficient, $\frac{QDOT}{TO - TW}, \frac{\text{Btu}}{\text{ft}^2\text{-sec-°R}}$
HI/HU	Ratio of interference to non-interference heat transfer coefficient, based on H(RTO)
H(0.90TO)	Heat-transfer coefficient, $\frac{QDOT}{(0.90TO)-TW}, \frac{\text{Btu}}{\text{ft}^2\text{-sec-°R}}$

H(0.95TO) — Heat-transfer coefficient, $\frac{QDOT}{(0.95TO)-TW}$, $\frac{Btu}{ft^2\text{-sec-}^\circ R}$

H(RTO) — Heat-transfer coefficient, $\frac{QDOT}{(RTO)-TW}$, $\frac{Btu}{ft^2\text{-sec-}^\circ R}$

HREF, HREF-FR — Reference heat-transfer coefficient based on Fay-Riddell theory, $Btu/ft^2\text{-sec-}^\circ R$

$$HREF = \left[\frac{8.1717\ (PO1)^{0.5}(MU\text{-}0)^{0.4}[1-(P\text{-}INF/PO1)]^{0.25}}{(RN)^{0.5}\ (TO)^{0.15}}\right] \times\ [0.2235 + 0.0000135\ [TO + 560]]$$

where PO1 ~ stagnation pressure downstream of a normal shock, psia

MU-0 ~ air viscosity based on TO, $lbf\text{-sec}/ft^2$

RN ~ reference nose radius, (0.0275 ft)

L — Axial reference length, (50.752 in.)

MACH NO., M_∞ — Free-stream Mach number

MODEL — Model configuration

MU-INF — Free-stream viscosity, $lbf\text{-sec}/ft^2$

P-INF — Free-stream pressure, psia

PO, P_o — Tunnel stilling chamber pressure, psia

QDOT — Heat-transfer rate, wbc_p (DTWDT), $Btu/ft^2\text{-sec}$

Q-INF — Free-stream dynamic pressure, psia

r — Recovery factor

R — Analytical temperature ratio, TAW/TO (see Section 3.4)

RE/FT, Re_∞ — Free-stream Reynolds number per foot, ft^{-1}

RHO-INF — Free-stream density, $slug/ft^3$

ROLL-MODEL — Model roll angle, positive for clockwise rotation looking upstream (=0 for $\theta = 0$ facing top of tunnel), deg

STFR	Theoretical stagnation point Stanton number for a 0.0275-ft (1 scale foot) radius sphere calculated from Fay-Riddell theory

$$STFR = \frac{HREF}{(RHO\text{-}INF)(V\text{-}INF)[0.2235 + 0.0000135(TO + 560)](32.174)}$$

SWITCH POSITION	Designates the position of the thermocouple selector switch
t	Time from start of model injection cycle, sec
T	Temperature, °R
TAW	Adiabatic wall temperature, °R
TC-NO(T/C)	Thermocouple Number
T-INF, T_∞	Free-stream temperature, °R
TO, T_o	Tunnel stilling chamber temperature, °R
TW	Model wall temperature, °R
V-INF	Free-stream velocity, ft/sec
w	Model wall density, lbm/ft^3
x_m	Model axial distance measured from 10-deg cone apex (see Fig. 3b), in.
X/L	Thermocouple axial location ratioed to the reference length, L ($X/L = x_m/L - 0.0027$)
YAW	Model yaw angle, deg
β	Angle of sideslip, equal to negative yaw angle, deg
γ	Ratio of specific heat, 1.4 for air
δ	Local surface angle of attack, deg
ϵ	Combination of model roll angle and θ, deg
θ, THETA	External tank angular measurement, deg
λ	Local model deflection angle, deg

SUBSCRIPTS

e	Flow properties at boundary layer edge
i	Initial conditions
∞	Free-stream flow properties

1.0 INTRODUCTION

The work reported herein was conducted by the Arnold Engineering Development Center (AEDC), Air Force Systems Command (AFSC), under program Element 921E01, Control Number 9E01-00-8, at the request of the National Aeronautics and Space Administration, Johnson Space Center (NASA/JSC) for the Martin-Marietta Aerospace Co. (MMA), New Orleans, Louisiana. The NASA/JSC project monitor was Mrs. Dorothy B. Lee, with Mr. John Warmbrod of Marshall Space Flight Center as the test monitor. The MMA project monitor was Mr. Harry Carroll. The test results were obtained by ARO, Inc., AEDC Division (a Sverdrup Corporation Company), operating contractor for the AEDC, AFSC, Arnold Air Force Station, Tennessee. The test was conducted in the von Karman Gas Dynamics Facility (VKF), Supersonic Wind Tunnel (A) under Project No. V41A-20. The test period was from May 1-5, 1978. Copies of the final data were sent to NASA and MMA on June 2, 1978 in the form of a Final Data Package. Requests for copies of the data should be sent to NASA/JSC. A microfilm record will be retained permanently within the VKF and one printed copy will be retained temporarily.

The primary test objective was to obtain heat-transfer distributions on the forward 23 percent of the Space Shuttle External Tank (ET). Specific objectives were: (1) to determine the change in heating, if any, due to the small change in the nose spike and (2) to measure the interference heating on the surface around the forward fairing, trays, gaseous oxygen (GOX) line and brackets, for comparison with, "clean body" heating data.

The test was conducted using the thin-skin thermocouple technique to obtain the heat-transfer data, and selected flow field information were obtained using shadowgraph and oil flow photographs. Data were obtained at Mach numbers 3, 4 and 5.5; and at free stream Reynolds numbers of 3.7 and 5.0 million per ft. Model angle of attack was 0, and ±5 deg, with sideslip angles from -11 to +11 deg.

2.0 APPARATUS

2.1 WIND TUNNEL

Tunnel A is a continuous, closed-circuit, variable density wind tunnel with an automatically driven flexible-plate-type nozzle and a 40- by 40-in. test section. The tunnel can be operated at Mach numbers from 1.5 to 6 at maximum stagnation pressures from 29 to 200 psia, respectively, and stagnation temperatures up to 750°R (M_∞ = 6). Minimum operating pressures range from about one-tenth to one-twentieth of the maximum at each Mach number. The tunnel is equipped with a model injection system which allows removal of the model from the test section while the tunnel remains in operation. A description of the tunnel and airflow calibration information may be found in Ref. 1. A schematic view of Tunnel A and the model injection system is shown in Fig. 1, Appendix A.

2.2 MODEL

The ET Forebody model used for the present test was a 0.0275-scale model of the forward 23 percent of the Space Shuttle External Tank which was designed by Rockwell International. Model design and fabrication was performed by Martin Marietta Aerospace with details given in Martin drawing WT7508001. The model was constructed of 304 stainless steel with a skin thickness of 0.030 in., ±0.0005 (per fabrication specifications) at the instrumented areas. Skin thickness spot check measurements were made at the VKF using an ultrasonic thickness measuring instrument. Excellent agreement was noted, typically within 0.001 in. All thermocouples were spot welded to the thin-skin inner surface. Model photographs are presented in Fig. 2 and the basic model geometry is defined in Fig. 3. A sketch of the model installation is shown in Fig. 4.

Two configurations were tested, one with all hardware (ET NOSE) on, the other with the hardware removed (ET NOSE/CLEAN). Boundary layer trips were added during the test to verify that the boundary layer was naturally turbulent. The trips were formed from either twisted wires or commerical carborundum grit. Two 0.004-in. diam wires were twisted together and spot welded to the model surface for the first type of trip. The second type of trip was formed with #60 carborundum grit, about 1/4-in wide. In each case the trip was located just behind the fairing.

2.3 INSTRUMENTATION AND MEASUREMENT ACCURACY

Tunnel A stilling chamber pressure is measured with a 15, 60, 150, or a 300-psid transducer referenced to a near vacuum. Based on periodic comparisons with secondary standards, the accuracy (a bandwidth which includes 95 percent of the residuals i.e. 2σ deviation) of these transducers is estimated to be within ±0.2 percent of reading or ±0.015 psia, whichever is greater. Stilling chamber temperature is measured with a copper-constantan thermocouple with an accuracy of ±3°F based on repeat calibrations (2σ deviation).

The model was instrumented with 250 Chromel®-constantan thermocouples with locations illustrated in Fig. 5, and their dimensional locations given in Table 1. All thermocouples were spot welded to the thin-skin inner surface.

The data were recorded using the Digital Equipment Corp.® PDP-11 and DEC-10 Computers in conjunction with a Beckman® 210 analog-to-digital converter. Data from a maximum of 97 thermocouples can be recorded during each tunnel injection. However, three switch positions provided the capability to record data from all 250 thermocouples during three tunnel injections.

3.0 TEST DESCRIPTION

3.1 TEST CONDITIONS

The test was conducted in Tunnel A at nominal Mach numbers of 3, 4, and 5.5 and free-stream unit Reynolds numbers of 3.7 and 5.0 million per ft. Data were taken at model angle-of-attack values of -5, 0, and 5 deg, with sideslip angles from -11 to 11 deg. The nominal tunnel test conditions are listed below, while a complete test summary showing all configurations tested, and the variables for each, is presented in Table 2.

M_∞	p_o, psia	T_o*, °R	HREF, $\frac{Btu}{ft^2\text{-sec-}°R}$	$Re_\infty \times 10^{-6}$, ft^{-1}
3.01	36	720	0.056	3.7
4.02	65,63	740,720	0.049	↓
5.5	127	720	0.039	↓
5.5	174,172	730,720	0.046	5.0

* Compressor plant inlet temperature limitations required reducing stagnation temperature below the level requested by the user and project engineer. Tunnel stagnation pressure was adjusted to maintain the same Re_∞.

3.2 TEST PROCEDURE

The initial step prior to recording the test data was to cool the model to approximately 40°F with cooled high pressure air. The cooling manifold was retracted from the model and the model attitude was established prior to injection. The thermocouple outputs were scanned approximately 17 times per second starting prior to model injection into the air-stream and continuing about 5 seconds after the model reached tunnel centerline. When the model reached tunnel centerline the model was immediately translated forward. After each injection, the cooling cycle was repeated to cool the model to an isothermal state.

3.3 DATA REDUCTION

The reduction of thin-skin thermocouple data normally involves only the calorimeteric heat balance which in coefficient form is:

$$H(TAW) = wbc_p \frac{dTW/dt}{TAW-TW} \tag{1}$$

For this test a value of 0.95 TO (based on experience) was selected for TAW and equation (1) can be written

$$H(0.95TO) = wbc_p \frac{dTW/dt}{0.95TO-TW} \tag{2}$$

Radiation and conduction losses are neglected in this heat balance and data reduction simply requires evaluation of dTW/dt from the temperature-time data and determination of model material properties. For the present tests, radiation effects were negligible; however, conduction effects can be significant in several regions of the model. To permit identification of these reqions and to improve evaluation of the data, the following procedure was used.

Separation of variables and integration of equation (2) assuming constant w, b, c_p, and TO yields

$$\frac{H(0.95TO)}{wbc_p} (t - t_i) = \ln\left[\frac{0.95TO - TW_i}{0.95TO - TW}\right] \tag{3}$$

Differentiation of Eq. (3) with respect to time gives

$$\frac{H(0.95TO)}{wbc_p} = \frac{d}{dt} \ln\left[\frac{0.95TO - TW_i}{0.95TO - TW}\right] \tag{4}$$

Since the left side of Eq. (4) is a constant, plotting $\ln\left[\frac{0.95TO - TW_i}{0.95TO - TW}\right]$ versus time will give a straight line if conduction is negligible. Thus, deviation from a straight line can be interpreted as conduction effects.

The data were evaluated in this manner, and generally a linear portion of the curve was used for all thermocouples. A linear least-square curve fit of $\ell n\ [(0.95TO-TW_1)/(0.95TO-TW)]$ versus time was applied to the data. Data reduction was started as soon as the model reached the tunnel centerline and the curve fit extended for a time span which was a function of the heating rate, as shown in the following list.

Range	No. of Points (Fit Length)
$\frac{dTW}{dt} > 32$	5
$16 < \frac{dTW}{dt} \leq 32$	7
$8 < \frac{dTW}{dt} \leq 16$	9
$4 < \frac{dTW}{dt} \leq 8$	13
$2 < \frac{dTW}{dt} \leq 4$	17
$1 < \frac{dTW}{dt} \leq 2$	25
$\frac{dTW}{dt} \leq 1$	41

The above time spans were generally adequate to keep the evaluation of the right side of Eq. (4) within the linear region. The linearity of the fit was substantiated by visual inspection of the cases in question. This visual check of the data was done on the VKF graphics terminal. Strictly speaking, the value of c_p for the material was not constant, and the following relation

$$c_p = 0.0825 + (6.5 \times 10^{-5})\ TW,\ \text{(304 stainless steel) Btu/lbm-°R} \qquad (5)$$

was used with the value of TW at the midpoint of the curve fit. The maximum variation of c_p over any curve fit was less than 0.5 percent.

The value of density used for 304 stainless steel was $w = 488.0$ lbm/ft^3, and the skin thickness, b, was 0.030 in.

3.4 ADIABATIC WALL TEMPERATURE

The maximum available tunnel stagnation temperature for each Mach number tested is listed in Section 3.1. With these relatively low stagnation temperatures, the difference between the model wall temperature and recovery temperature was generally small in regions of peak heating. This small temperature difference causes the calculation of the heat-transfer coefficient to be very sensitive to deviations from the actual adiabatic wall temperature. Two values of the heat-transfer coefficient have been calculated based on an assumed constant recovery temperature, namely H(TO) and H(0.90TO). To account for changes in the recovery temperature a third value of the heat-transfer coefficient has been tabulated based on an analytical temperature ratio, R = TAW/TO.

The analytical method for determining R was developed by Rockwell International and has been used to calculate H(RTO). In this method, the following relationships were assumed:

$$R = \frac{TAW}{TO} \tag{6}$$

and

$$TAW = T_e \left(1 + \frac{\gamma-1}{2} r M_e^2\right) \tag{7}$$

$$r = 0.898 \text{ for turbulent flow}$$

with r being the recovery factor and the subscript e identifying local properties at the boundary-layer edge. From these relationships, the temperature ratio can be defined as:

$$R = \frac{1 + 0.2 r M_e^2}{1 + 0.2 M_e^2} \tag{8}$$

which is a function of the recovery factor and the local Mach number. The local Mach number can be written

$$M_e = M_e(M_\infty, \delta) \tag{9}$$

where ∞ identifies the free-stream property and δ is the local surface angle of attack.

The local Mach number can be approximated by using tangent cone flow theory, and was used in Equation (8) to give R as a function of M_∞ and δ. Calculations of R were made for several values of M_∞ and δ, and the results were curve fit by Rockwell International. The following equation resulted

$$R(M_\infty, \delta) = a_1 + a_2 \cdot (\sin \delta)^{a_3} \tag{10}$$

where a_1, a_2, a_3 are constants for a particular Mach number. The values of a_1, a_2, a_3 used for this test are:

M_∞	a_1	a_2	a_3
3.0	0.9345	0.1004	2.165
4.0	0.922	0.1004	1.965
5.5	0.910	0.1004	1.686

Standard matrix techniques, Ref. 2, were used to derive the following relations for δ, as applicable to the model geometry.

$$\delta = \arcsin (\sin \lambda \cos \alpha_s + \cos \lambda \cos \varepsilon \sin \alpha_s) \tag{11}$$

where $\alpha_s \equiv$ alpha-sector, deg

$\varepsilon \equiv$ roll model + (θ +180), deg

$\lambda \equiv$ local model deflection angle, deg

$\lambda = \sin^{-1}\left(\frac{12.062 - x_m}{16.876}\right)$, deg for thermocouple on the ogive section $x_m > 1.355$ in. ($X/L > 0.0238$)

$\lambda = 39.38$ deg for thermocouples on the cone section, $x_m \leq 1.355$ in. ($X/L \leq 0.0238$)

$\lambda = 55$ deg for all thermocouples on the fairing

The method used to calculate the analytical temperature ratio, R, has been applied to all of the tabulated data. The method represents a simplified approach to present a more realistic evaluation of TAW. However, in regions of separated flow or complex interaction, the values calculated for R may no longer apply and should be used with extreme care.

4.0 PRECISION OF MEASUREMENTS

The accuracy of the basic measurements (p_o and T_o) was discussed in Section 2.3. Based on repeat calibrations, these errors were found to be

$$\frac{\Delta p_o}{p_o} = 0.002 = 0.2\%, \quad \frac{\Delta T_o}{T_o} = 0.005 = 0.5\%$$

Uncertainties in the tunnel free-stream parameters and the model aerodynamic coefficients were estimated using the Taylor series method of error propagation, Eq. (12)

$$(\Delta F)^2 = \left(\frac{\partial F}{\partial X_1}\Delta X_1\right)^2 + \left(\frac{\partial F}{\partial X_2}\Delta X_2\right)^2 + \left(\frac{\partial F}{\partial X_3}\Delta X_3\right)^2 \ldots + \left(\frac{\partial F}{\partial X_n}\Delta X_n\right)^2 \qquad (12)$$

where ΔF is the absolute uncertainty in the dependent parameter $F = F(X_1, X_2, X_3 \ldots X_n)$ and X_n is the independent parameter (or basic measurement). ΔX_n is the uncertainty (error) in the independent measurement (or variable).

4.1 Test Conditions

The accuracy (based on 2σ deviation) of the basic tunnel parameters, p_o and T_o, (see Section 2.3) and the 2σ deviation in Mach number determined from test section flow calibrations were used to estimate uncertainties

in the other free-stream properties using Eq.(12). The computed uncertainties in the tunnel free-stream conditions are summarized in the following table.

	Uncertainty, (±) percent of actual value			
M_∞	M_∞	p_∞	q_∞	Re_∞
3.01	0.6	2.6	1.4	1.2
4.01	0.4	2.4	1.5	1.2
5.50	0.3	1.9	1.3	1.1

The uncertainty in model angle of attack and sideslip angle as determined from calibrations is estimated to be ±0.2 deg.

4.2 DATA

Estimated uncertainties for the individual terms in Eq. (2) were used in the Taylor series method of error propagation to obtain uncertainty in values of heat-transfer coefficient as given below:

H(TO), $\frac{Btu}{ft^2\text{-sec-}^\circ R}$	Uncertainty, (±) percent
10^{-4}	10
10^{-3}	7
10^{-2}	5

The data were deleted from the results for thermocouples which consistently exceeded the above quoted uncertainties.

5.0 DATA PACKAGE PRESENTATION

Detailed heat-transfer rate distributions were obtained on a 0.0275-scale forebody model of the space shuttle external tank. Two configurations were tested, one with all hardware on, the other with the hardware removed. The standard configuration (hardware on) data can be compared directly to the clean model data, thereby providing a ratio of interference heating to undisturbed heating.

Shadowgraph pictures were taken during many model injections and two oil flow Groups were made at the end of the test program.

Data verification is best determined by comparing data from the clean model (no hardware) to appropriate analytical solutions. Because of the complex geometry of even the clean model, no truly accurate analytic modeling can be computed for the nose area. However, theory (Ref. 3) for a cone-ogive-cylinder at zero incidence is shown compared to the present data in Fig. 6. The agreement is considered adequate. A typical interference heating ratio plot is shown in Fig. 7. Typical tabulated data are shown in Fig. 8.

REFERENCES

1. Test Facilities Handbook (Tenth Edition). "von Karman Gas Dynamics Facility, Vol. 4." Arnold Engineering Development Center, May 1974.

2. Trimmer, L. L. and Clark, E. L. "Transformation of Axes Systems by Matrix Methods and Applications to Wind Tunnel Data Reduction." AEDC-TDR-63-224, October 1963.

3. Mayne, A. W., Jr. "A Method for Computing Boundary Layer Flows, Including Normal Pressure Gradients and Longitudinal Curvature Effects," AEDC-TR-75-21 (ADA008739), April 1975.

APPENDIX A

ILLUSTRATIONS

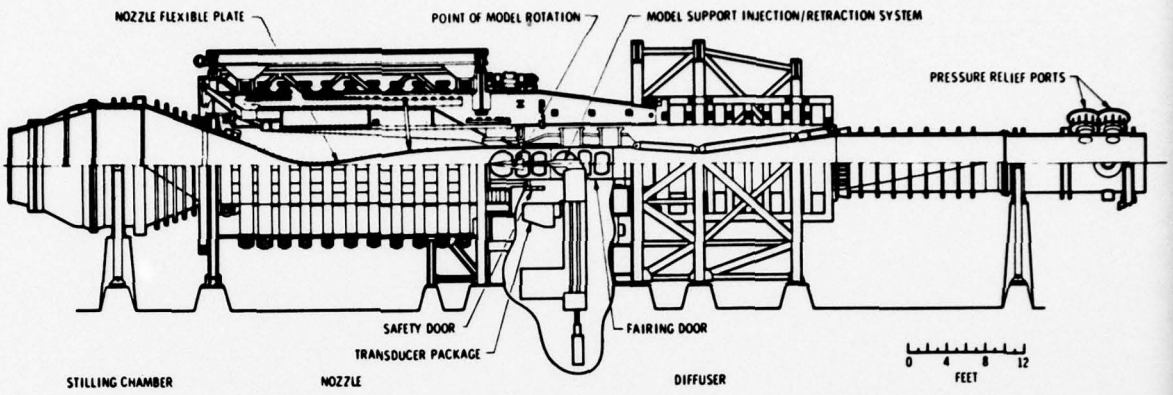

a. Tunnel assembly

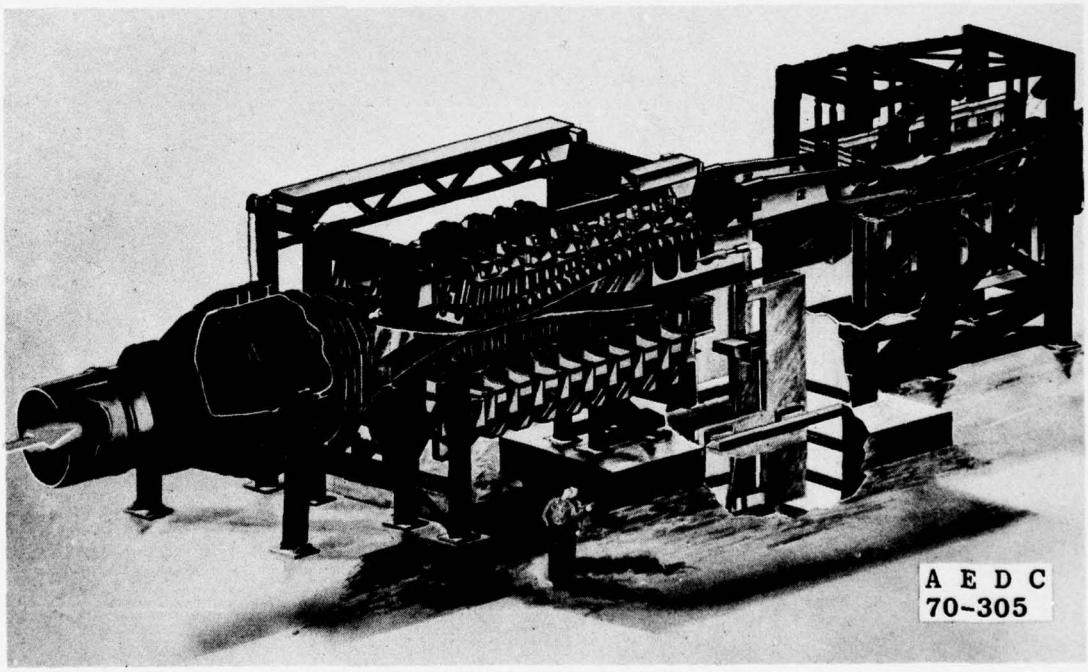

b. Tunnel test section

Fig. 1 Tunnel A

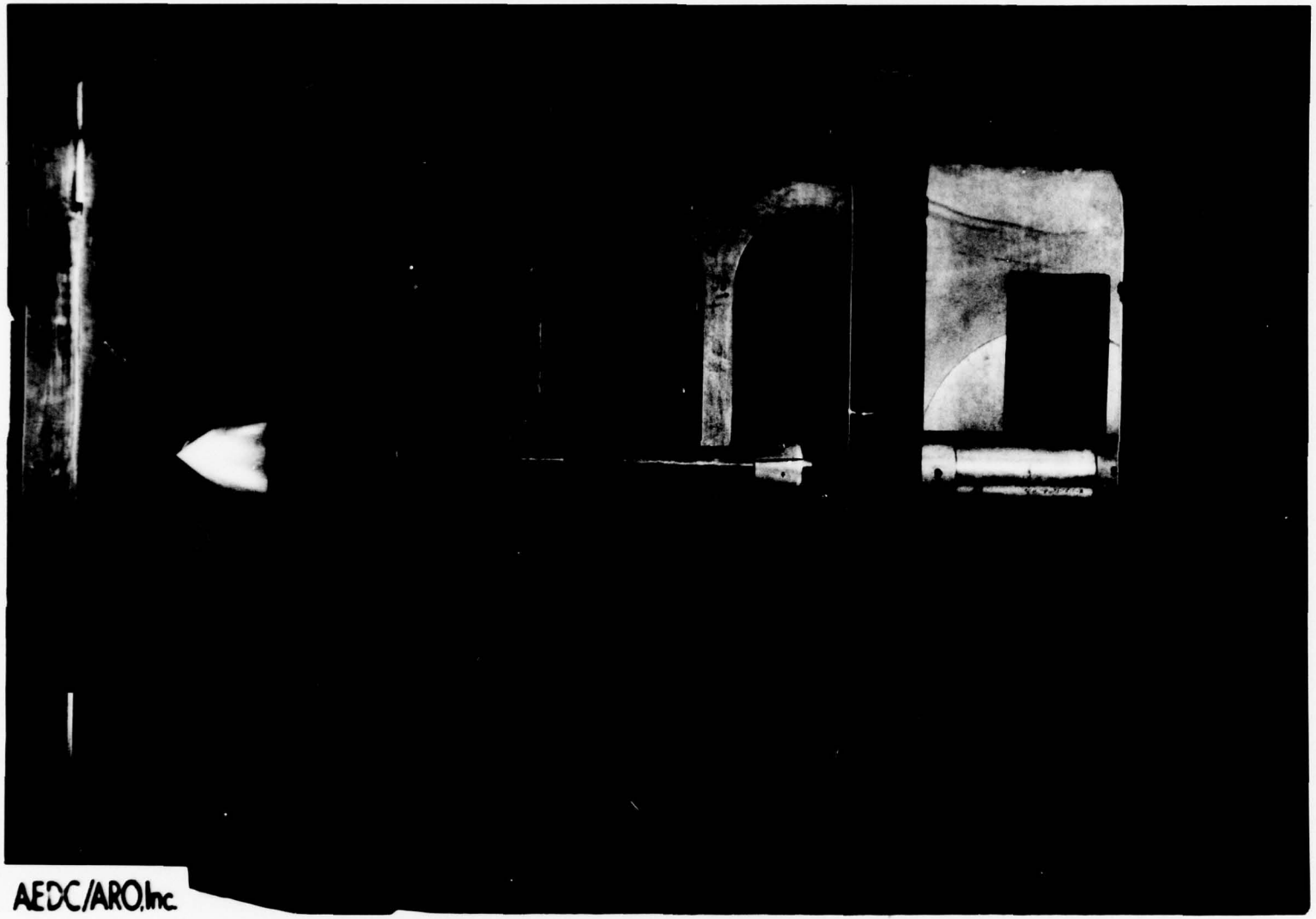

a. Profile View in Tunnel A
Figure 2. Model Photographs

b. Front View
Figure 2. Concluded

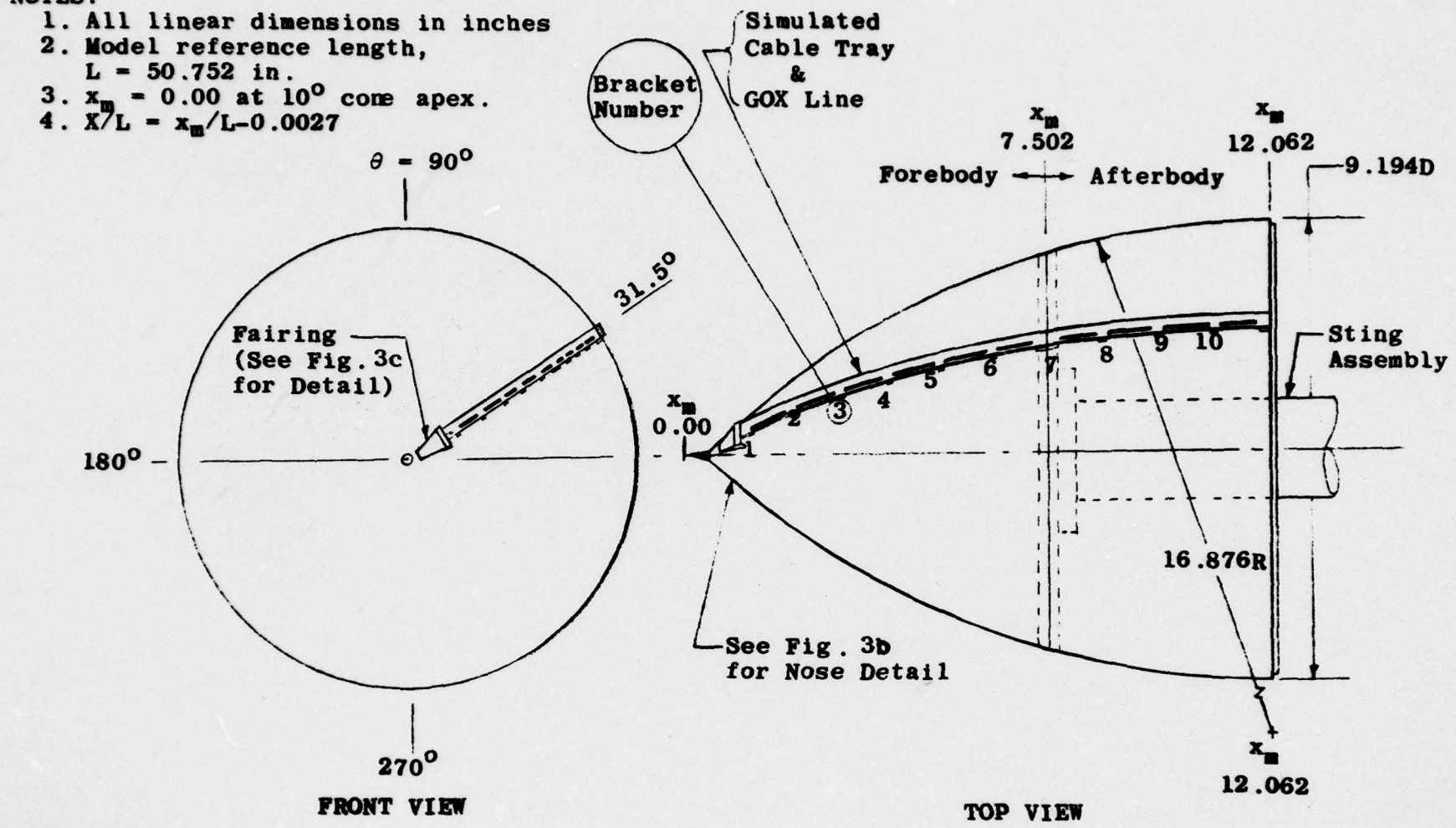

a. Overall Geometry

Figure 3. Model Geometry

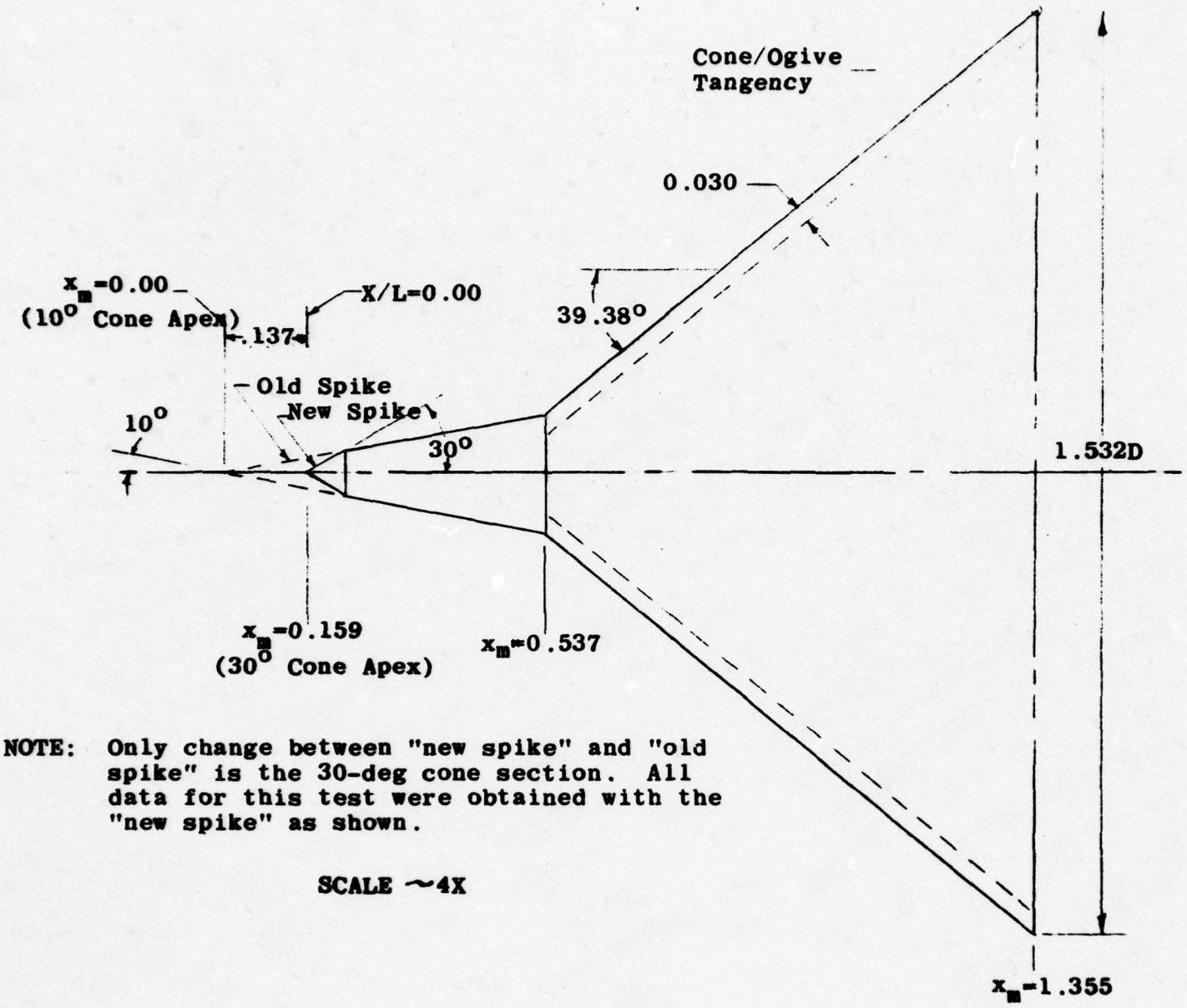

NOTE: Only change between "new spike" and "old spike" is the 30-deg cone section. All data for this test were obtained with the "new spike" as shown.

SCALE ~4X

b. Nose Detail

Figure 3. Continued

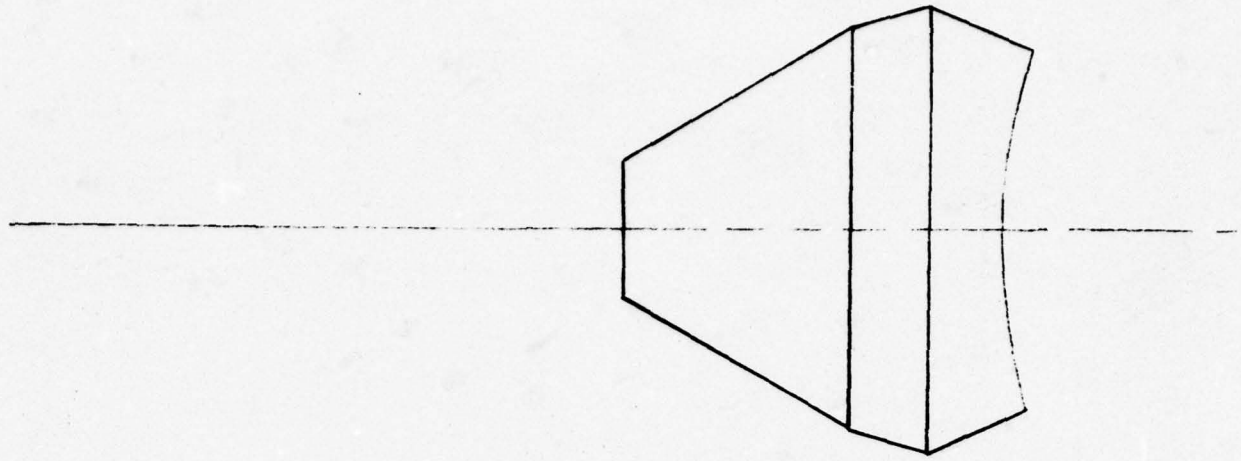

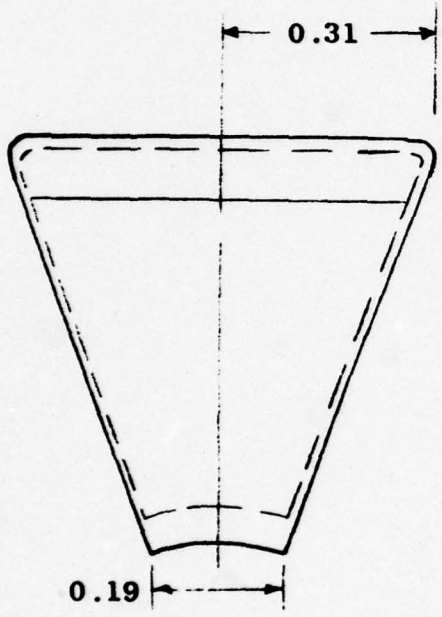

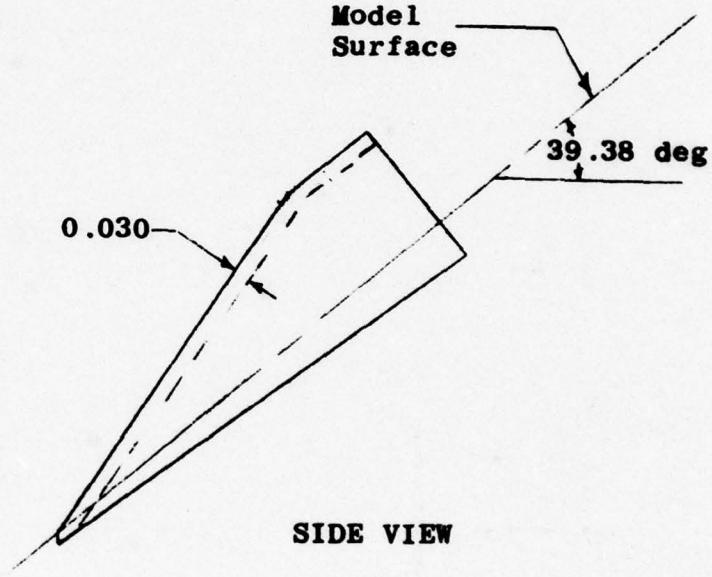

c. Fairing

Figure 3. Concluded

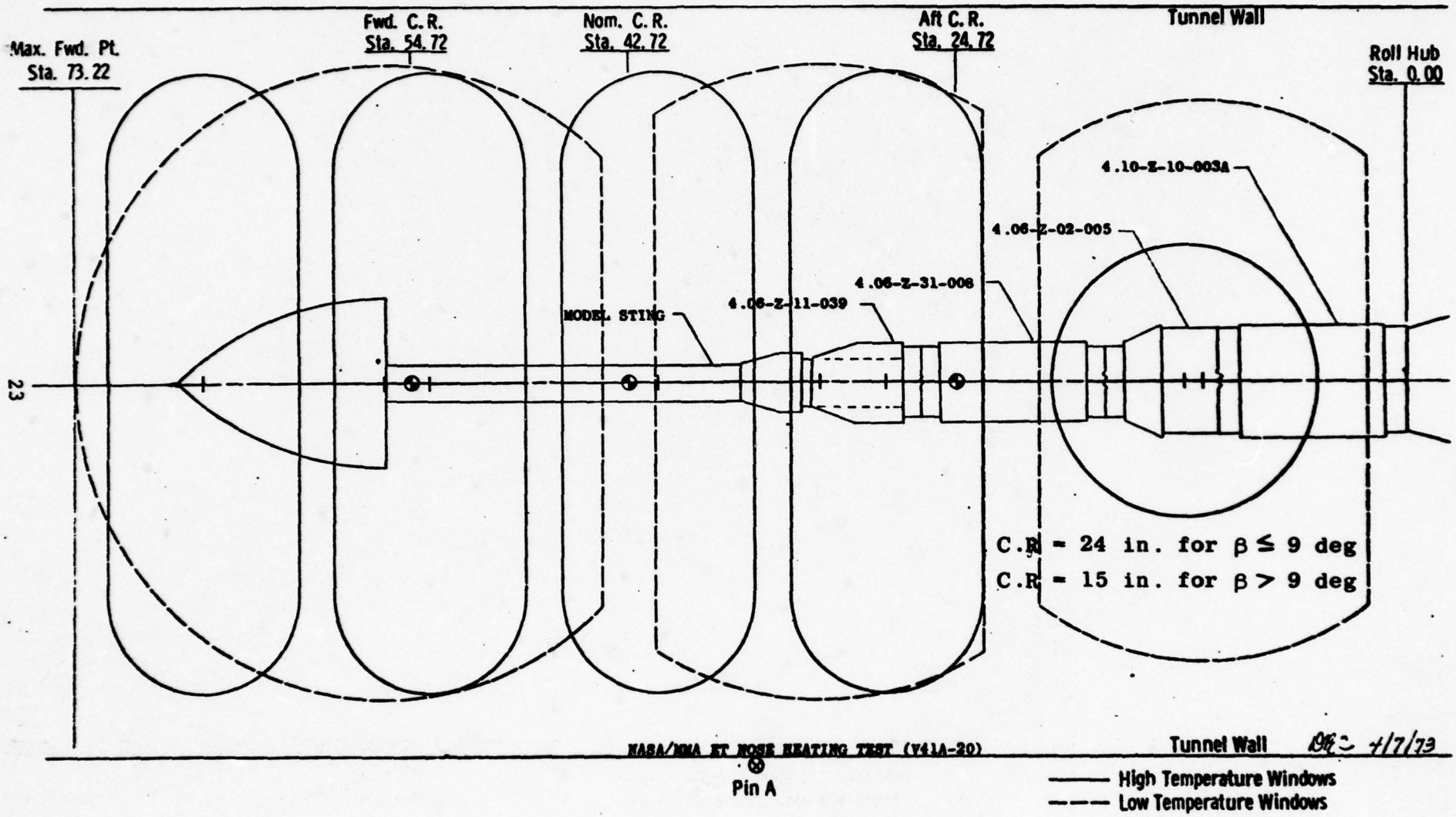

Figure 4. Model Installation Sketch

Notes: 1. See Table 1 for Coordinate Informatic

2. Thermocouples in the Vicinity of the Fairing, Cable Tray and GOX Line are Shown in Figures 5b thru 5g

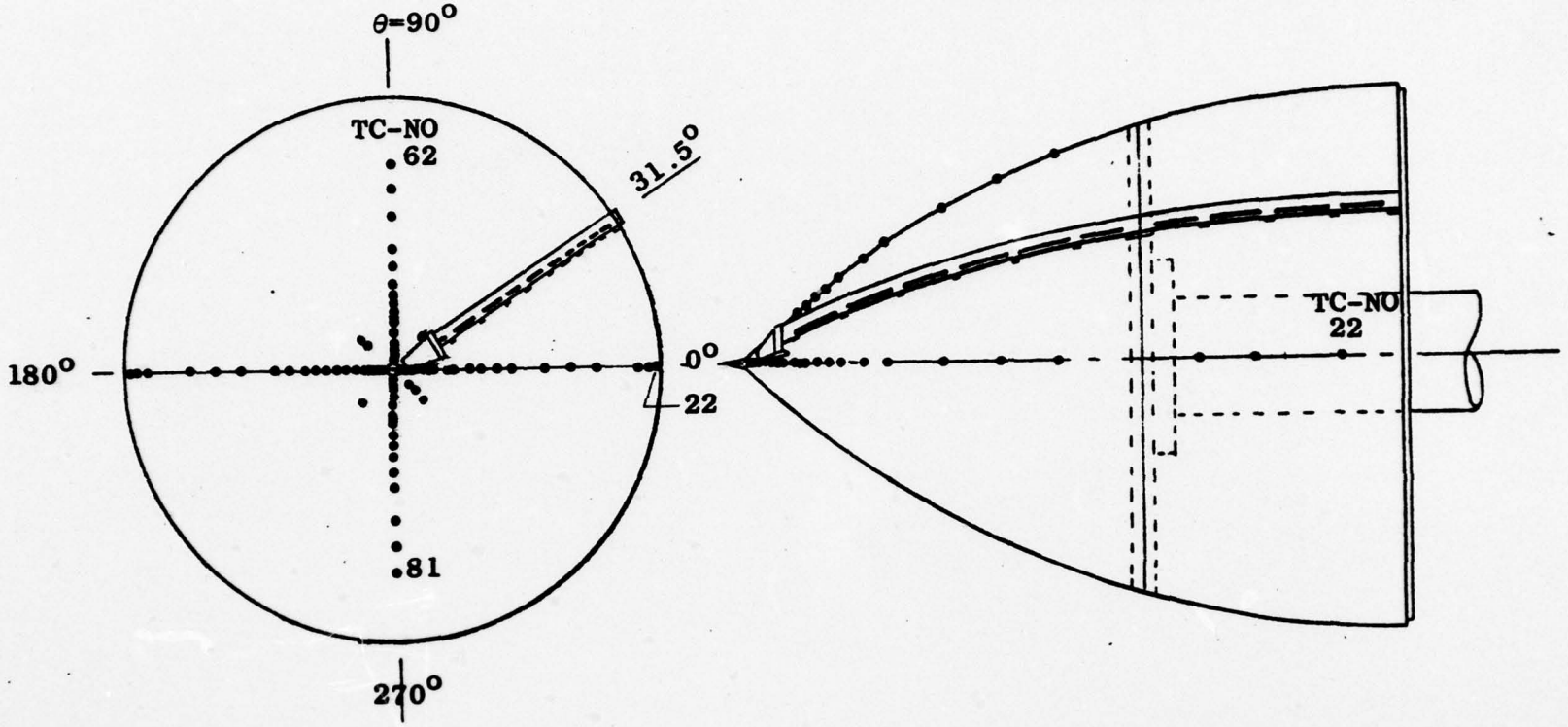

a. Constant θ Lines

Figure 5. Thermocouple Locations

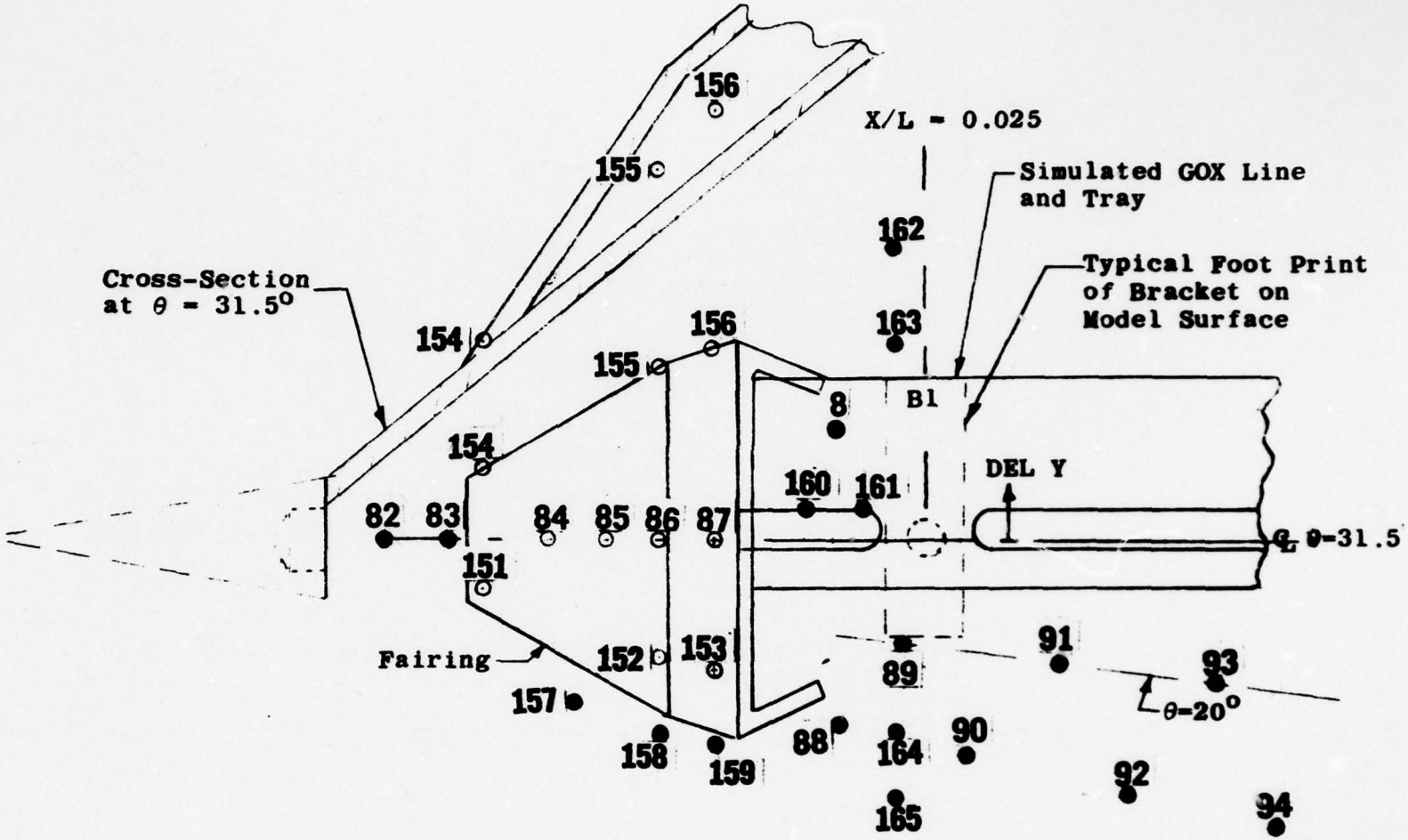

EXPANDED VIEW ~4X SIZE

b. Thermocouples on Fairing and Near GOX Line and Tray/Bracket B1

Figure 5. Continued

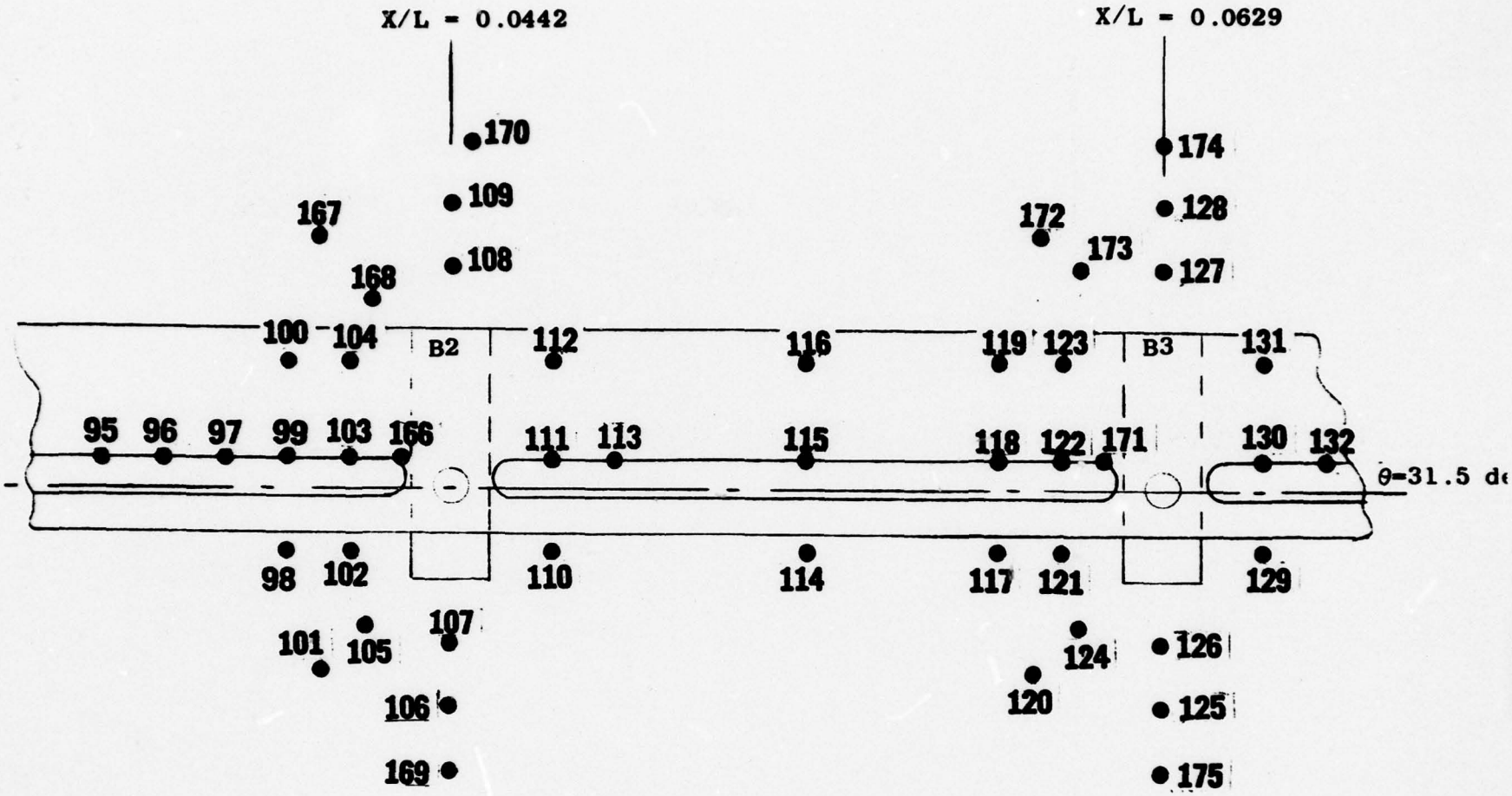

EXPANDED VIEW ~ 4X SIZE

c. Thermocouples Near GOX Line and Tray/Brackets B2 and B3

Figure 5. Continued

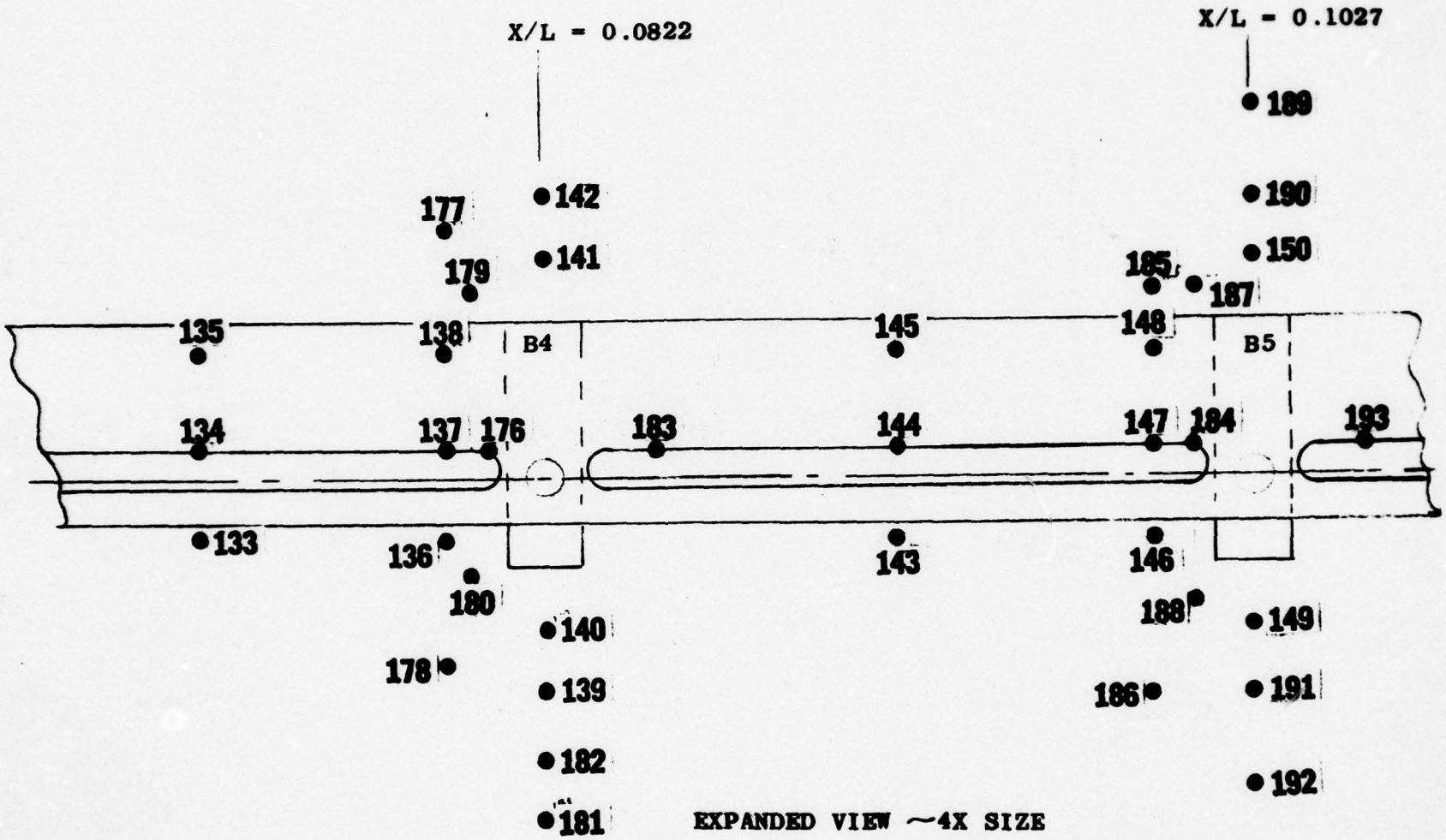

d. Thermocouples Near GOX Line and Tray/Brackets B4 and B5

Figure 5. Continued

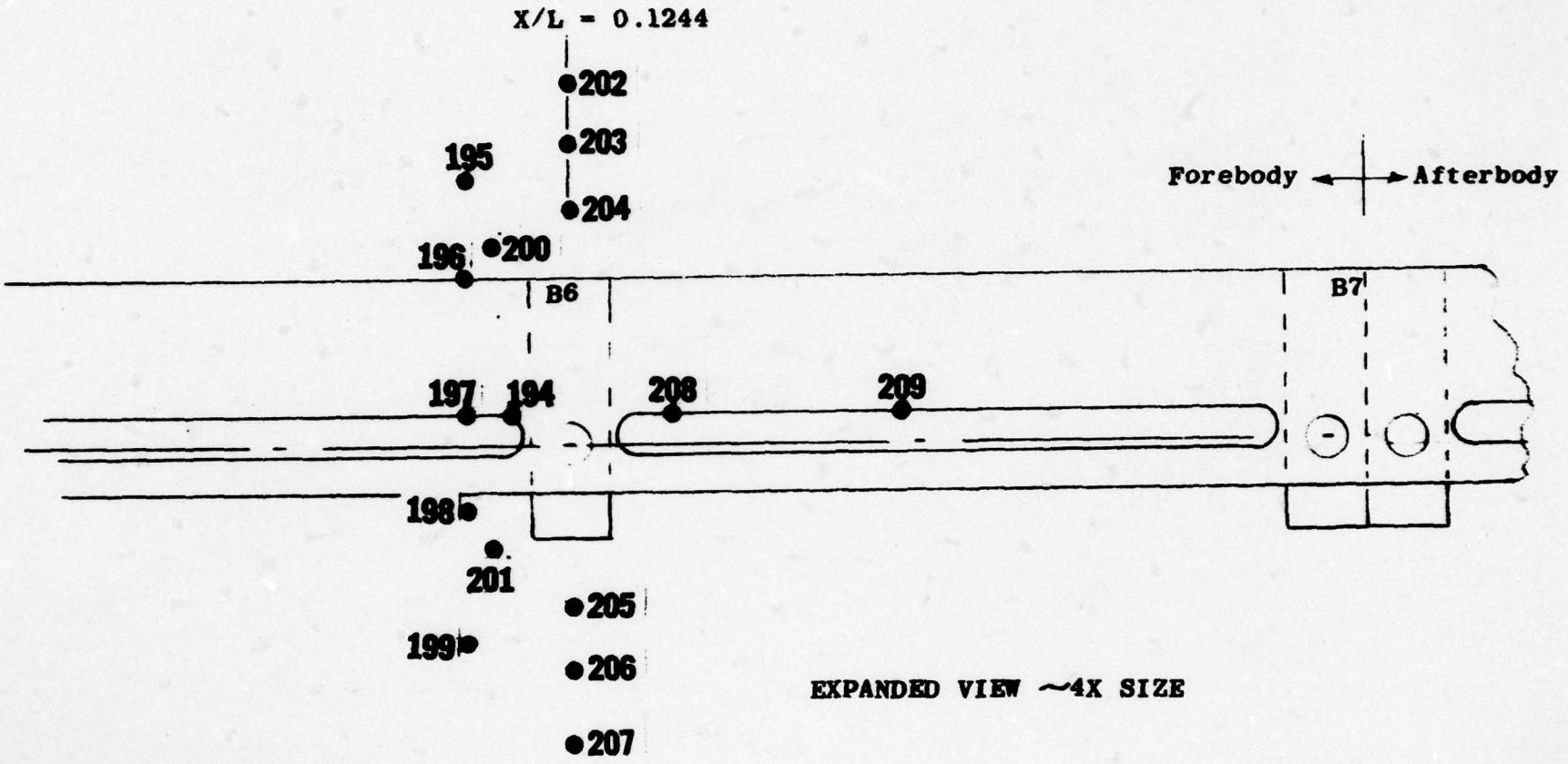

e. Thermocouples Near GOX Line and Tray/Bracket B6

Figure 5. Continued

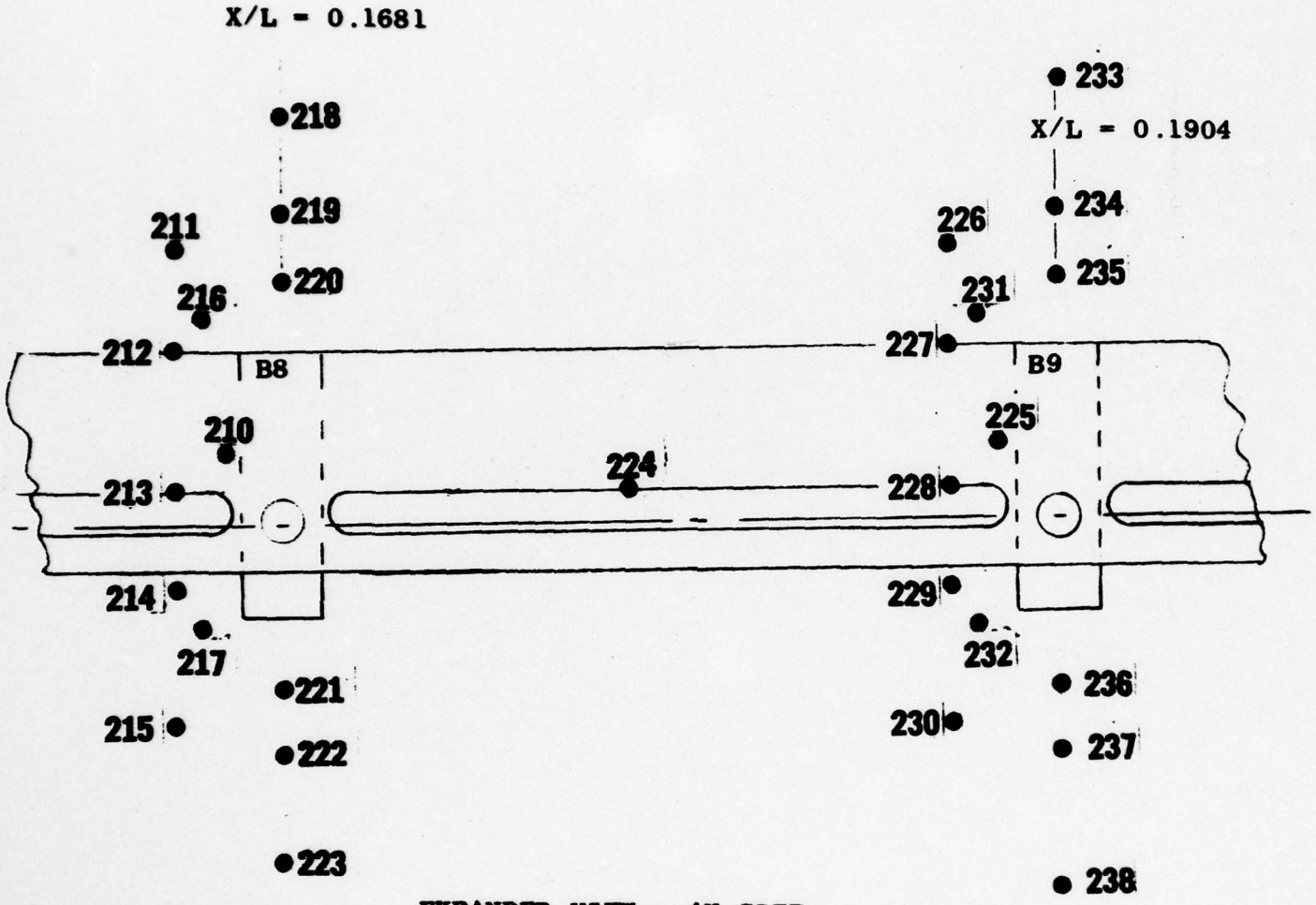

EXPANDED VIEW ~4X SIZE

f. Thermocouples Near GOX Line and Tray/Brackets B8 and B9

Figure 5. Continued

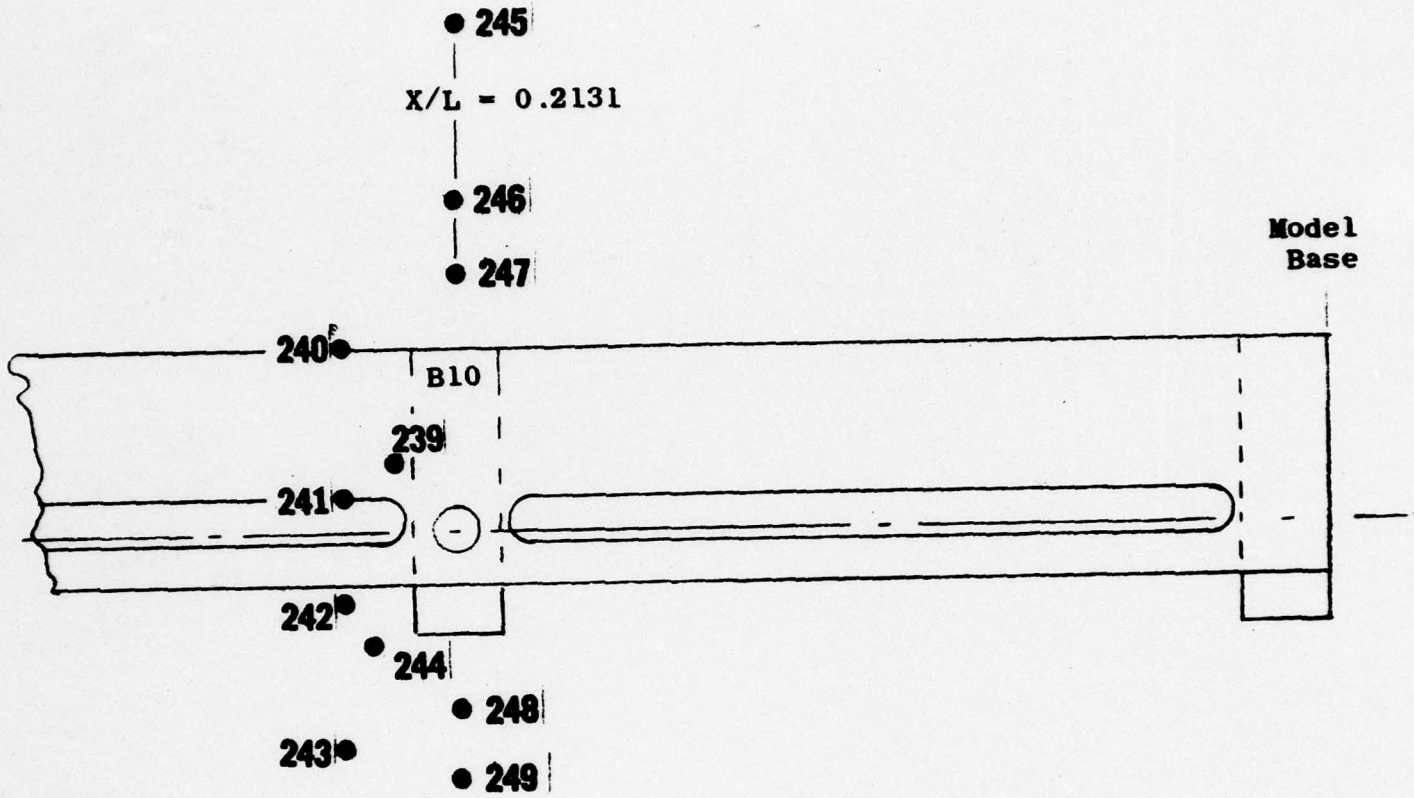

g. Thermocouples Near GOX Line and Tray/Bracket B10

Figure 5. Concluded

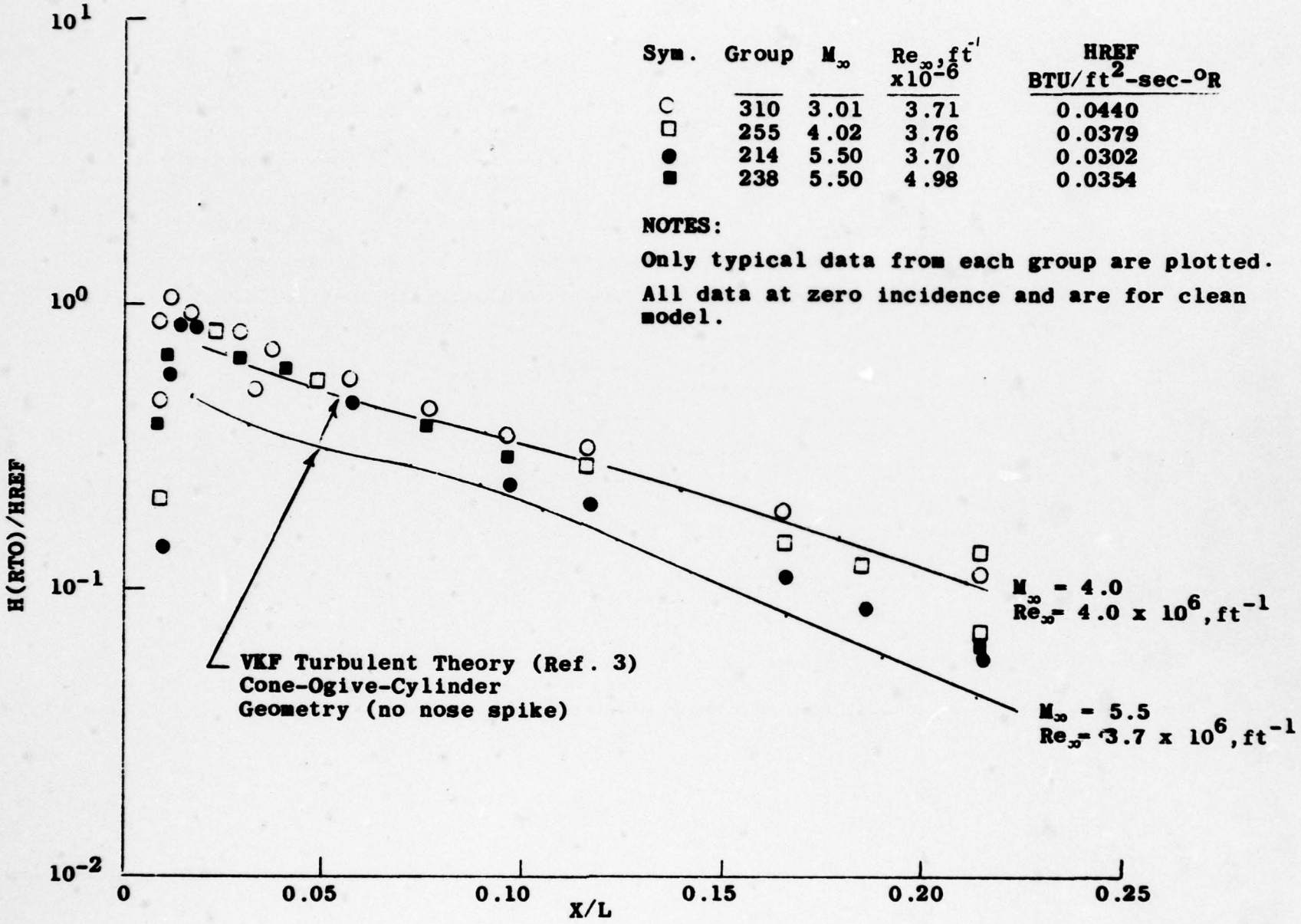

Figure 6. Data Verification Plot

NOTES:

Data from groups 73 and 257.

See Fig. 5e and 5f for thermocouple location and model geometry.

M_∞ = 4.02

Re_∞ = 3.71 x 10^6, ft^{-1}

Model at zero incidence

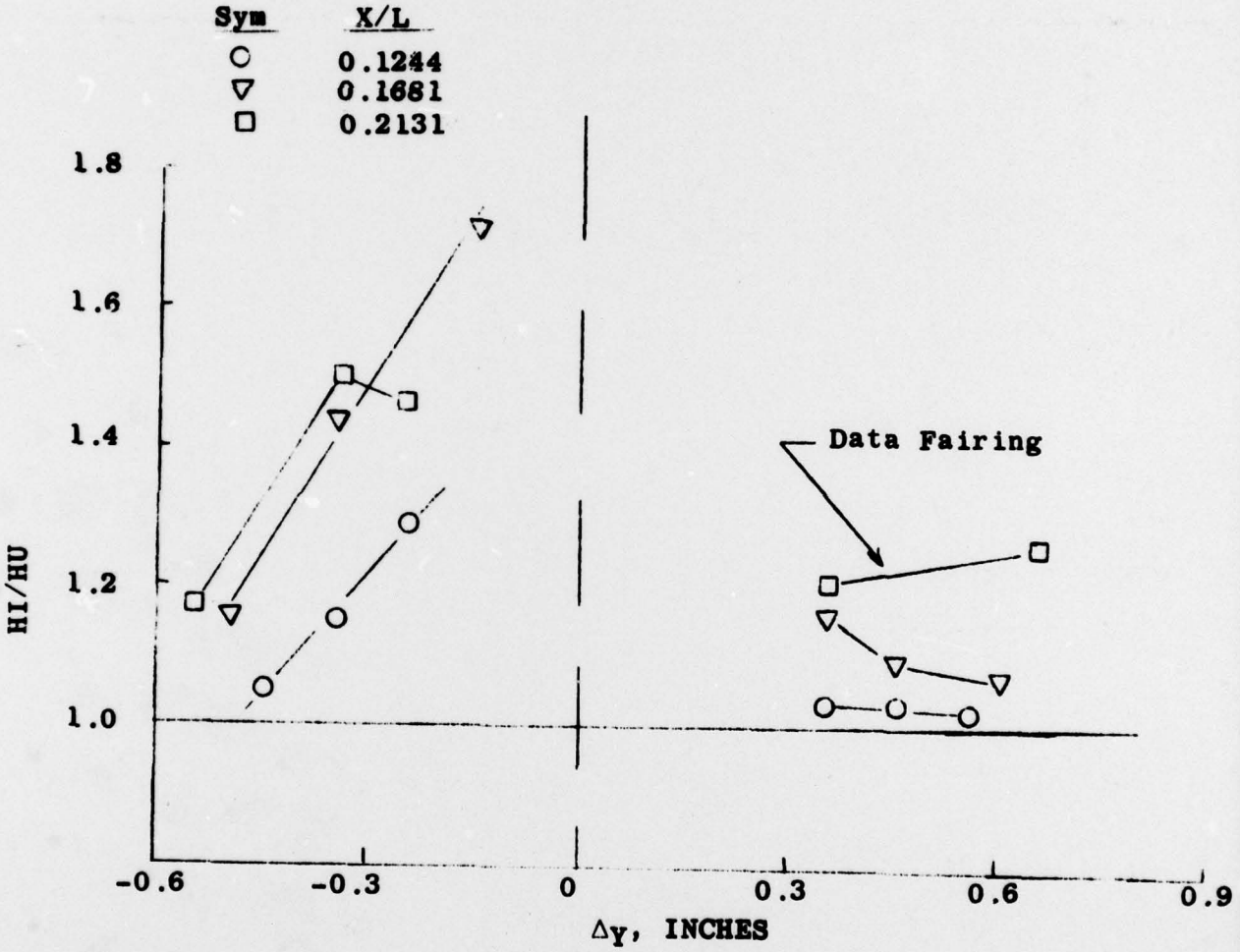

Figure 7. Typical Interference Heating

ARO, INC. - AEDC DIVISION
A SVERDRUP CORPORATION COMPANY
VON KARMAN GAS DYNAMICS FACILITY
ARNOLD AIR FORCE STATION, TENNESSEE
NASA/MSA (FM15) ET NOSE HEATING TES T

DATE COMPUTED 26-MAY-78
TIME COMPUTED 06:32:24
DATE RECORDED 2-MAY-78
TIME RECORDED 7:41: 8
PROJECT NUMBER V41A-20

GROUP	CONFIG	MODEL	MACH NO	PO,PSIA	TO,DEG R	ALPHA-MODEL	ALPHA-SECTOR	ALPHA-PREBEND	ROLL-MODEL	YAW	CR
94	1	ET NOSE	4.02	65.1	739.7	-5.01	-7.81	0.	50.28	6.00	24.09

T-INF (DEGR)	P-INF (PSIA)	Q-INF (PSIA)	V-INF (FT-SEC)	RHO-INF (LBM/FT3)	MU-INF (LB-SEC/FT2)	RE/FT (FT-1)	HREF-FR (RN= 0.0275FT)	STFR (RN= 0.0275FT)	SWITCH POSITION
174.78	0.42	4.723	2605.	6.447E-03	1.406E-07	3.712E+06	3.88E-02	9.572E-03	3

TC-NO	TW	DT*DT	QDOT	H(TO)	H(TO)/HREF	H(.90TO)	H(.90TO)/HREF	P	H(RTO)	H(RTO)/HREF	EXT. TANK X/L	EXT. TANK THETA	EXT. TANK DEL Y
161	535.5	18.797	2.690	0.132E-01	0.3399	0.207E-01	0.5330	0.9632	0.152E-01	0.3921	0.0239	35.2	0.05
162	561.7	22.992	3.337	0.187E-01	0.4837	0.321E-01	0.8277	0.9564	0.229E-01	0.5907	0.0247	65.2	0.45
163	545.5	20.569	2.967	0.156E-01	0.4032	0.256E-01	0.6606	0.9589	0.186E-01	0.4802	0.0247	53.2	0.40
164	559.8	23.286	3.378	0.198E-01	0.4846	0.319E-01	0.8231	0.9688	0.215E-01	0.5560	0.0247	9.8	-0.30
165	557.2	22.930	3.320	0.182E-01	0.4693	0.306E-01	0.7892	0.9704	0.207E-01	0.5333	0.0247	2.0	-0.40
166	565.2	29.144	4.280	0.277E-01	0.7159	0.532E-01	1.3737	0.9588	0.350E-01	0.9024	0.0428	33.4	0.05
167	559.4	22.407	3.250	0.180E-01	0.4657	0.306E-01	0.7903	0.9543	0.222E-01	0.5731	0.0408	47.7	0.40
168	557.3	21.113	3.058	0.166E-01	0.4326	0.282E-01	0.7278	0.9549	0.205E-01	0.5294	0.0420	43.2	0.30
169	561.6	25.115	3.646	0.205E-01	0.5283	0.350E-01	0.9035	0.9606	0.245E-01	0.6318	0.0442	14.6	-0.45
170	545.5	19.376	2.644	0.136E-01	0.3515	0.220E-01	0.5678	0.9521	0.167E-01	0.4299	0.0448	51.9	0.55
171	549.1	24.501	3.613	0.242E-01	0.6232	0.478E-01	1.2330	0.9508	0.319E-01	0.8234	0.0613	32.9	0.05
172	549.4	26.859	3.916	0.230E-01	0.5935	0.407E-01	1.0494	0.9493	0.295E-01	0.7612	0.0596	42.6	0.40
173	566.3	24.146	3.515	0.203E-01	0.5232	0.354E-01	0.9127	0.9493	0.259E-01	0.6678	0.0607	41.1	0.35
174	569.0	25.526	3.722	0.219E-01	0.5647	0.387E-01	0.9992	0.9476	0.283E-01	0.7315	0.0629	46.1	0.55
175	559.1	22.547	3.284	0.182E-01	0.4693	0.308E-01	0.7951	0.9532	0.225E-01	0.5807	0.0629	19.6	-0.45
176	575.2	21.133	3.091	0.198E-01	0.4849	0.342E-01	0.8812	0.9451	0.250E-01	0.6440	0.0808	32.6	0.05
177	568.6	24.758	3.608	0.211E-01	0.5444	0.372E-01	0.9592	0.9439	0.278E-01	0.7186	0.0795	40.1	0.40
178	562.6	22.350	3.247	0.183E-01	0.4732	0.315E-01	0.8126	0.9470	0.236E-01	0.6078	0.0795	25.0	-0.30
179	567.1	23.340	3.399	0.197E-01	0.5082	0.345E-01	0.8896	0.9441	0.259E-01	0.6682	0.0803	38.0	0.30
180	570.1	26.556	3.876	0.229E-01	0.5895	0.405E-01	1.0456	0.9463	0.296E-01	0.7699	0.0803	27.2	-0.20
181	550.4	15.480	2.234	0.118E-01	0.3045	0.194E-01	0.4998	0.9426	0.152E-01	0.3926	0.0822	43.4	0.55
182	556.4	19.597	2.837	0.155E-01	0.3994	0.259E-01	0.6695	0.9468	0.197E-01	0.5085	0.0822	21.8	-0.45
183	536.4	11.216	1.606	0.790E-02	0.2038	0.124E-01	0.3204	0.9437	0.993E-02	0.2564	0.0858	32.5	0.05
184	573.5	18.304	2.675	0.161E-01	0.4153	0.290E-01	0.7483	0.9397	0.220E-01	0.5676	0.1011	32.4	0.05
185	562.2	18.252	2.651	0.149E-01	0.3853	0.256E-01	0.6606	0.9388	0.200E-01	0.5171	0.1000	38.7	0.40
186	561.6	18.169	2.661	0.146E-01	0.3826	0.254E-01	0.6543	0.9413	0.196E-01	0.5059	0.1000	25.3	-0.35
187	567.6	16.499	2.403	0.140E-01	0.3604	0.245E-01	0.6323	0.9389	0.189E-01	0.4869	0.1011	36.9	0.30
188	571.5	20.996	3.065	0.182E-01	0.4702	0.325E-01	0.8394	0.9405	0.247E-01	0.6368	0.1011	27.9	-0.20
189	565.3	15.631	2.262	0.123E-01	0.3165	0.205E-01	0.5285	0.9376	0.164E-01	0.4223	0.1027	42.3	0.60
190	562.9	18.957	2.754	0.156E-01	0.4019	0.268E-01	0.6910	0.9380	0.210E-01	0.5426	0.1027	39.5	0.45
191	555.6	18.699	2.706	0.147E-01	0.3793	0.246E-01	0.6340	0.9406	0.193E-01	0.4982	0.1027	25.3	-0.35
192	550.5	14.824	2.139	0.113E-01	0.2917	0.186E-01	0.4790	0.9411	0.147E-01	0.3790	0.1027	22.6	-0.50
193	533.6	10.117	1.446	0.702E-02	0.1811	0.109E-01	0.2825	0.9384	0.901E-02	0.2325	0.1063	32.4	0.05
194	575.4	13.611	2.020	0.123E-01	0.3173	0.224E-01	0.5771	0.9347	0.174E-01	0.4495	0.1230	32.3	0.05
195	560.0	14.783	2.144	0.119E-01	0.3079	0.203E-01	0.5233	0.9342	0.164E-01	0.4222	0.1210	37.9	0.40
196	567.4	13.924	2.013	0.117E-01	0.3017	0.205E-01	0.5267	0.9346	0.163E-01	0.4195	0.1210	35.5	0.25
197	571.8	16.664	2.433	0.145E-01	0.3739	0.259E-01	0.6684	0.9351	0.203E-01	0.5236	0.1210	32.3	0.05
198	579.8	18.974	2.782	0.174E-01	0.4490	0.324E-01	0.8356	0.9355	0.248E-01	0.6400	0.1210	29.9	-0.10
199	573.7	18.892	2.761	0.166E-01	0.4293	0.300E-01	0.7746	0.9360	0.233E-01	0.6007	0.1210	26.7	-0.30
200	564.9	12.319	1.792	0.103E-01	0.2646	0.178E-01	0.4589	0.9343	0.142E-01	0.3667	0.1220	36.3	0.30
201	561.7	14.579	2.117	0.119E-01	0.3068	0.203E-01	0.5250	0.9355	0.162E-01	0.4191	0.1220	28.3	-0.20
202	557.9	12.481	1.805	0.993E-02	0.2564	0.168E-01	0.4323	0.9332	0.136E-01	0.3521	0.1244	40.2	0.55
203	558.4	12.397	1.797	0.991E-02	0.2557	0.167E-01	0.4319	0.9334	0.136E-01	0.3511	0.1244	38.6	0.45
204	558.0	11.129	1.613	0.888E-02	0.2291	0.150E-01	0.3865	0.9337	0.122E-01	0.3139	0.1244	37.0	0.35
205	566.5	16.002	2.329	0.134E-01	0.3470	0.228E-01	0.5857	0.9381	0.186E-01	0.4800	0.1244	27.6	-0.25

ARO, INC. - AEDC DIVISION
A SVERDRUP CORPORATION COMPANY
VON KARMAN GAS DYNAMICS FACILITY
ARNOLD AIR FORCE STATION, TENNESSEE
NASA/MMA (Fm15) ET NOSE HEATING TES T

DATE COMPUTED 26-MAY-78
TIME COMPUTED 06:32:24
DATE RECORDED 2-MAY-78
TIME RECORDED 7:41: 8
PROJECT NUMBER V41A-28

GROUP	CONFIG	MODEL	MACH NO	PO,PSIA	TO,DEG R	ALPHA-MODEL	ALPHA-SECTOR	ALPHA-PREBEND	ROLL-MODEL	YAW	CR
94	1	ET NOSE	4.02	65.1	739.7	-5.01	-7.81	0.	50.28	6.00	24.39

T-INF (DEGR)	P-INF (PSIA)	Q-INF (PSIA)	V-INF (FT-SEC)	RHO-INF (LBM/FT3)	MU-INF (LB-SEC/FT2)	RE/FT (FT-1)	HREF-FR (RN= 0.0275FT)	STFR (RN= 0.0275FT)	SWITCH POSITION
174.78	0.42	4.723	2605.	6.447E-03	1.406E-07	3.712E+06	3.88E-02	9.572E-03	3

TC-NO	TW	DTWDT	QDOT	H(TO)	H(TO)/HREF	H(.90TO)	H(.90TO)/HREF	R	H(RTO)	H(RTO)/HREF	EXT. TANK X/L	THETA	DEL Y
206	559.8	13.244	1.921	0.107E-01	0.2755	0.181E-01	0.4679	0.9354	0.145E-01	0.3752	0.1244	24.0	-0.35
207	555.7	10.563	1.526	0.831E-02	0.2144	0.139E-01	0.3586	0.9356	0.112E-01	0.2892	0.1244	24.4	-0.45
208	546.3	7.372	1.061	0.549E-02	0.1416	0.889E-02	0.2293	0.9338	0.735E-02	0.1896	0.1273	32.3	0.05
209	541.4	8.481	1.231	0.691E-02	0.1783	0.118E-01	0.3047	0.9324	0.960E-02	0.2477	0.1342	32.3	0.05
210	553.6	9.502	1.374	0.739E-02	0.1906	0.123E-01	0.3163	0.9270	0.104E-01	0.2684	0.1668	32.8	0.10
211	555.7	10.016	1.450	0.782E-02	0.2034	0.137E-01	0.3402	0.9269	0.112E-01	0.2881	0.1648	36.9	0.40
212	556.0	8.989	1.303	0.717E-02	0.1850	0.121E-01	0.3121	0.9271	0.102E-01	0.2631	0.1648	34.9	0.25
213	561.2	11.352	1.648	0.923E-02	0.2383	0.158E-01	0.4069	0.9274	0.132E-01	0.3409	0.1648	32.2	0.05
214	565.5	14.337	2.086	0.120E-01	0.3091	0.206E-01	0.5372	0.9276	0.173E-01	0.4463	0.1649	30.2	-0.10
215	554.9	10.542	1.528	0.827E-02	0.2134	0.138E-01	0.3558	0.9279	0.116E-01	0.3000	0.1648	27.4	-0.30
216	554.7	8.778	1.276	0.686E-02	0.1771	0.114E-01	0.2951	0.9269	0.970E-02	0.2503	0.1650	35.6	0.30
217	560.6	13.162	1.910	0.107E-01	0.2753	0.182E-01	0.4692	0.9276	0.152E-01	0.3929	0.1658	28.8	-0.20
218	547.9	7.762	1.118	0.583E-02	0.1505	0.949E-02	0.2450	0.9262	0.815E-02	0.2104	0.1681	39.6	0.60
219	547.6	8.661	1.246	0.650E-02	0.1676	0.106E-01	0.2727	0.9264	0.907E-02	0.2340	0.1681	37.6	0.45
220	548.4	8.124	1.171	0.612E-02	0.1580	0.998E-02	0.2576	0.9265	0.855E-02	0.2207	0.1681	36.2	0.35
221	552.6	12.745	1.841	0.984E-02	0.2540	0.163E-01	0.4200	0.9273	0.138E-01	0.3563	0.1661	28.2	-0.25
222	545.6	9.964	1.419	0.731E-02	0.1867	0.118E-01	0.3049	0.9275	0.101E-01	0.2607	0.1681	26.8	-0.35
223	541.9	6.867	0.996	0.496E-02	0.1286	0.796E-02	0.2053	0.9277	0.683E-02	0.1762	0.1681	24.8	-0.53
224	535.7	8.566	1.226	0.601E-02	0.1551	0.943E-02	0.2434	0.9256	0.823E-02	0.2124	0.1786	32.2	0.05
225	525.1	6.124	0.872	0.406E-02	0.1049	0.620E-02	0.1601	0.9245	0.550E-02	0.1418	0.1888	32.8	0.10
226	536.6	7.528	1.078	0.531E-02	0.1370	0.835E-02	0.2155	0.9244	0.733E-02	0.1891	0.1870	36.7	0.40
227	540.5	7.976	1.145	0.575E-02	0.1484	0.915E-02	0.2360	0.9245	0.799E-02	0.2062	0.1870	34.7	0.25
228	536.5	6.559	0.939	0.462E-02	0.1193	0.727E-02	0.1875	0.9247	0.637E-02	0.1643	0.1870	32.2	0.05
229	533.1	10.600	1.552	0.790E-02	0.2038	0.127E-01	0.3267	0.9249	0.110E-01	0.2841	0.1870	30.2	-0.10
230	532.8	8.276	1.183	0.572E-02	0.1475	0.890E-02	0.2296	0.9251	0.781E-02	0.2015	0.1870	27.6	-0.30
231	537.0	5.912	0.847	0.418E-02	0.1078	0.656E-02	0.1697	0.9244	0.577E-02	0.1489	0.1888	35.4	0.30
232	DELETE												
233	531.4	5.788	0.827	0.396E-02	0.1026	0.617E-02	0.1593	0.9239	0.546E-02	0.1408	0.1904	39.9	0.65
234	DELETE												
235	531.9	5.758	0.822	0.396E-02	0.1022	0.615E-02	0.1587	0.9241	0.542E-02	0.1400	0.1904	36.0	0.35
236	530.0	10.314	1.472	0.702E-02	0.1811	0.108E-01	0.2799	0.9247	0.956E-02	0.2467	0.1904	28.3	-0.25
237	529.8	7.977	1.138	0.542E-02	0.1399	0.837E-02	0.2161	0.9248	0.738E-02	0.1904	0.1904	27.0	-0.35
238	522.6	5.197	0.738	0.340E-02	0.0878	0.516E-02	0.1331	0.9250	0.457E-02	0.1179	0.1904	24.4	-0.55
239	DELETE												
240	530.5	4.614	0.659	0.315E-02	0.0813	0.487E-02	0.1257	0.9228	0.433E-02	0.1116	0.2101	34.7	0.25
241	534.4	5.972	0.854	0.416E-02	0.1073	0.650E-02	0.1678	0.9229	0.576E-02	0.1486	0.2101	32.1	0.05
242	536.4	8.966	1.284	0.632E-02	0.1630	0.993E-02	0.2563	0.9230	0.878E-02	0.2265	0.2101	30.3	-0.10
243	526.5	7.432	1.059	0.502E-02	0.1294	0.772E-02	0.1992	0.9231	0.686E-02	0.1771	0.2101	27.7	-0.30
244	529.7	8.098	1.155	0.550E-02	0.1420	0.849E-02	0.2192	0.9230	0.755E-02	0.1946	0.2111	29.8	-0.20
245	524.7	4.243	0.604	0.281E-02	0.0725	0.429E-02	0.1105	0.9224	0.383E-02	0.0989	0.2131	40.3	0.70
246	525.7	5.216	0.742	0.347E-02	0.0895	0.530E-02	0.1368	0.9225	0.474E-02	0.1223	0.2131	37.2	0.45
247	524.6	4.365	0.624	0.290E-02	0.0748	0.442E-02	0.1141	0.9226	0.395E-02	0.1020	0.2131	35.9	0.35
248	524.0	7.693	1.094	0.507E-02	0.1309	0.772E-02	0.1992	0.9229	0.690E-02	0.1779	0.2131	28.4	-0.25
249	521.6	6.535	0.928	0.426E-02	0.1100	0.645E-02	0.1665	0.9230	0.577E-02	0.1489	0.2131	27.1	-0.35
250	DELETE												

Figure 8. Concluded

APPENDIX B

TABLES

TABLE 1. THERMOCOUPLE DIMENSIONAL LOCATIONS

TC NO.	THETA	X/L	DEL Y
1	0.0000	0.0091	N/A
2	0.0000	0.0111	
3	0.0000	0.0131	
4	0.0000	0.0150	
5	0.0000	0.0170	
6	0.0000	0.0190	
7	0.0000	0.0209	
8	45.0000	0.0229	
9	0.0000	0.0249	
10	0.0000	0.0269	
11	0.0000	0.0288	
12	0.0000	0.0328	
13	0.0000	0.0367	
14	0.0000	0.0406	
15	0.0000	0.0485	
16	0.0000	0.0564	
17	0.0000	0.0761	
18	0.0000	0.0958	
19	0.0000	0.1155	
20	0.0000	0.1648	
21	0.0000	0.1845	
22	0.0000	0.2140	
23	180.0000	0.0091	
24	180.0000	0.0111	
25	180.0000	0.0131	
26	180.0000	0.0150	
27	180.0000	0.0170	
28	180.0000	0.0190	
29	180.0000	0.0209	N/A
30	225.0000	0.0229	
31	180.0000	0.0249	
32	180.0000	0.0288	
33	180.0000	0.0328	
34	180.0000	0.0367	
35	180.0000	0.0406	
36	180.0000	0.0485	
37	180.0000	0.0564	
38	180.0000	0.0761	
39	180.0000	0.0958	
40	180.0000	0.1155	
41	180.0000	0.1648	
42	180.0000	0.1845	
43	180.0000	0.2140	
44	90.0000	0.0091	
45	90.0000	0.0111	
46	90.0000	0.0131	
47	90.0000	0.0150	
48	90.0000	0.0170	
49	135.0000	0.0190	
50	90.0000	0.0209	
51	135.0000	0.0229	
52	90.0000	0.0249	
53	90.0000	0.0269	
54	90.0000	0.0288	
55	90.0000	0.0328	
56	90.0000	0.0367	

NOTES: Data were recorded on three different switch positions
Switch Position 1 - TC No. 12-81
Switch Position 2 - TC No. 1-11, 82-160
Switch Position 3 - TC No. 161-250
See Fig. 5b-5g for TC locations

TABLE 1. THERMOCOUPLE DIMENSIONAL LOCATIONS

TC NO.	THETA	X/L	DEL Y
57	90.0000	0.0406	N/A
58	90.0000	0.0485	
59	90.0000	0.0564	
60	90.0000	0.0761	
61	90.0000	0.0958	
62	90.0000	0.1155	
63	270.0000	0.0091	
64	270.0000	0.0111	
65	270.0000	0.0131	
66	315.0000	0.0150	
67	270.0000	0.0170	
68	315.0000	0.0190	
69	270.0000	0.0209	
70	315.0000	0.0229	
71	270.0000	0.0249	
72	270.0000	0.0269	
73	270.0000	0.0288	
74	270.0000	0.0328	
75	270.0000	0.0367	
76	270.0000	0.0406	
77	270.0000	0.0485	
78	270.0000	0.0564	
79	270.0000	0.0761	
80	270.0000	0.0958	
81	270.0000	0.1155	
82	31.5000	0.0091	
83	31.5000	0.0111	
84	31.5000	0.0142	
85	31.5000	0.0160	N/A
86	31.5000	0.0176	
87	31.5000	0.0194	
88	10.0000	0.0229	
89	20.0000	0.0249	
90	10.0000	0.0269	
91	20.0000	0.0288	
92	10.0000	0.0308	
93	20.0000	0.0328	
94	10.0000	0.0347	
95	33.9000	0.0338	0.0500
96	33.7000	0.0367	0.0500
97	33.6000	0.0383	0.0500
98	27.4000	0.0401	-0.1000
99	33.5000	0.0401	0.0500
100	39.7000	0.0401	0.2000
101	19.8000	0.0408	-0.2900
102	27.6000	0.0416	-0.1000
103	33.5000	0.0416	0.0500
104	39.3000	0.0416	0.2000
105	23.0000	0.0420	-0.2200
106	18.5000	0.0442	-0.3500
107	22.4000	0.0442	-0.2500
108	44.6000	0.0442	0.3500
109	48.4000	0.0442	0.4500
110	28.0000	0.0468	-0.1000
111	33.2000	0.0468	0.0500
112	38.5000	0.0468	0.3000

NOTES: Data were recorded on three different switch positions
Switch Position 1 - TC No. 12-81
Switch Position 2 - TC No. 1-11, 82-160
Switch Position 3 - TC No. 161-250
See Fig. 5b-5g for TC locations

TABLE 1. THERMOCOUPLE DIMENSIONAL LOCATIONS

TC NO.	THETA	X/L	DEL Y	TC NO.	THETA	X/L	DEL Y
113	33.2000	0.0483	0.0500	141	38.9000	0.0822	0.3500
114	28.4000	0.0535	-0.1000	142	41.1000	0.0822	0.4500
115	33.0000	0.0535	0.0500	143	29.6000	0.0925	-0.1000
116	37.6000	0.0535	0.2000	144	32.5000	0.0925	0.0500
117	28.7000	0.0586	-0.1000	145	35.3000	0.0925	0.2000
118	32.9000	0.0586	0.0500	146	29.7000	0.1000	-0.1000
119	37.1000	0.0586	0.2000	147	32.4000	0.1000	0.0500
120	23.4000	0.0596	-0.2900	148	35.1000	0.1000	0.2000
121	28.8000	0.0604	-0.1000	149	27.2000	0.1027	-0.2500
122	32.9000	0.0604	0.0500	150	37.8000	0.1027	0.3500
123	37.0000	0.0604	0.2000	151	12.0000	0.0121	9.0000
124	25.5000	0.0607	-0.2200	152	12.0000	0.0176	9.0000
125	22.2000	0.0629	-0.3500	153	13.0000	0.0194	9.0000
126	24.9000	0.0629	-0.2500	154	51.0000	0.0121	9.0000
127	40.9000	0.0629	0.3500	155	51.0000	0.0176	9.0000
128	43.6000	0.0629	0.4500	156	50.0000	0.0194	9.0000
129	29.0000	0.0657	-0.1000	157	9.0000	0.0150	9.0000
130	32.8000	0.0657	0.0500	158	9.0000	0.0176	9.0000
131	36.6000	0.0657	0.2000	159	9.0000	0.0194	9.0000
132	32.7000	0.0674	0.0500	160	35.3000	0.0221	0.0500
133	29.2000	0.0724	-0.1000	161	35.2000	0.0239	0.0500
134	32.7000	0.0724	0.0500	162	65.2000	0.0247	0.4500
135	36.2000	0.0724	0.2000	163	53.2000	0.0247	0.4000
136	29.3000	0.0795	-0.1000	164	9.8000	0.0247	-0.3000
137	32.6000	0.0795	0.0500	165	2.0000	0.0247	-0.4000
138	35.8000	0.0806	0.2000	166	33.4000	0.0428	0.0500
139	24.1000	0.0822	-0.3500	167	47.7000	0.0408	0.4000
140	26.3000	0.0822	-0.2500	168	43.2000	0.0420	0.3000

NOTES: Data were recorded on three different switch positions
Switch Position 1 - TC No. 12-81
Switch Position 2 - TC No. 1-11, 82-160
Switch Position 3 - TC No. 161-250
See Fig. 5b-5g for TC locations

TABLE 1. THERMOCOUPLE DIMENSIONAL LOCATIONS

TC NO.	THETA	X/L	DEL Y	TC NO.	THETA	X/L	DEL Y
169	14.6000	0.0442	-0.4500	197	32.3000	0.1210	0.0500
170	51.9000	0.0448	0.5500	198	29.9000	0.1210	-0.1000
171	32.9000	0.0613	0.0500	199	26.7000	0.1210	-0.3000
172	42.6000	0.0596	0.4000	200	36.3000	0.1220	0.3000
173	41.1000	0.0607	0.3500	201	26.3000	0.1220	-0.2000
174	46.1000	0.0629	0.5500	202	40.2000	0.1244	0.5500
175	19.6000	0.0629	-0.4500	203	38.6000	0.1244	0.4500
176	32.6000	0.0808	0.0500	204	37.0000	0.1244	0.3500
177	40.1000	0.0795	0.4000	205	27.6000	0.1244	-0.2500
178	25.0000	0.0795	-0.3000	206	26.0000	0.1244	-0.3500
179	39.9000	0.0803	0.3000	207	24.4000	0.1244	-0.4500
180	27.2000	0.0803	-0.2000	208	32.3000	0.1273	0.0500
181	43.4000	0.0822	0.5500	209	32.3000	0.1342	0.0500
182	21.8000	0.0822	-0.4500	210	32.8000	0.1668	0.1000
183	32.5000	0.0858	0.0500	211	36.9000	0.1648	0.4000
184	32.4000	0.1011	0.0500	212	34.9000	0.1648	0.2500
185	38.7000	0.1000	0.4000	213	32.2000	0.1648	0.0500
186	25.3000	0.1000	-0.3500	214	30.2000	0.1648	-0.1000
187	36.9000	0.1011	0.3000	215	27.4000	0.1648	-0.3000
188	27.9000	0.1011	-0.2000	216	35.6000	0.1658	0.3000
189	42.3000	0.1027	0.6000	217	28.8000	0.1658	-0.2000
190	39.5000	0.1027	0.4500	218	39.6000	0.1681	0.6000
191	25.3000	0.1027	-0.3500	219	37.6000	0.1681	0.4500
192	22.6000	0.1027	-0.5000	220	36.2000	0.1681	0.3500
193	32.4000	0.1063	0.0500	221	28.2000	0.1681	-0.2500
194	32.3000	0.1230	0.0500	222	26.8000	0.1681	-0.3500
195	37.9000	0.1210	0.4000	223	24.8000	0.1681	-0.5000
196	35.5000	0.1210	0.2500	224	32.2000	0.1786	0.0500

NOTES: Data were recorded on three different switch positions
Switch Position 1 - TC No. 12-81
Switch Position 2 - TC No. 1-11, 82-160
Switch Position 3 - TC No. 161-250
See Fig. 5b-5g for TC locations

TABLE 1. THERMOCOUPLE DIMENSIONAL LOCATIONS

TC NO.	THETA	X/L	DEL Y	TC NO.	THETA	X/L	DEL Y
225	32.4000	0.1888	0.1000				
226	36.7000	0.1870	0.4000				
227	34.7000	0.1870	0.2500				
228	32.2000	0.1870	0.0500				
229	30.2000	0.1870	-0.1000				
230	27.5000	0.1870	-0.3000				
231	35.4000	0.1880	0.3000				
232	28.4000	0.1880	-0.2000				
233	39.9000	0.1904	0.6500				
234	37.3000	0.1904	0.4500				
235	35.0000	0.1904	0.3500				
236	29.3000	0.1904	-0.2500				
237	27.0000	0.1904	-0.3500				
238	24.4000	0.1904	-0.5500				
239	32.4000	0.2117	0.1000				
240	34.7000	0.2101	0.2500				
241	32.1000	0.2101	0.0500				
242	30.4000	0.2101	-0.1000				
243	27.7000	0.2101	-0.3000				
244	29.0000	0.2111	-0.2000				
245	40.3000	0.2131	0.7000				
246	37.2000	0.2131	0.4500				
247	35.0000	0.2131	0.3500				
248	28.4000	0.2131	-0.2500				
249	27.1000	0.2131	-0.3500				
250	25.9000	0.2131	-0.6000				

NOTES: Data were recorded on three different switch positions
Switch Position 1 - TC No. 12-81
Switch Position 2 - TC No. 1-11, 82-160
Switch Position 3 - TC No. 161-250
See Fig. 5b-5g for TC locations

TABLE 2. TEST DATA SUMMARY

a. Protuberances on Model

M_∞	$Re_\infty \times 10^{-6}$, ft^{-1}	α, deg	β, deg									Sw. Pos.
			-11	-9	-6	-3	0	3	6	9	11	
3.0	3.7	-5			25	29	21,24‡	32	35			1
					26	30	22	33	36			2
					27	31	23	34	37			3
		0			6	12	2+, 5‡, 9+, 56+	15	28			1
					7	13	3+, 10+, 55+	16	19			2
					8	14	4+, 11+, 57+	17	20			3
		5			42	45	38,41‡	48	51			1
					43	46	39	49	52			2
					44	47	40	50	53			3
4.0		-5	112	115	92	96	88,91‡	99	102	105	111	1
			113	116	93	97	89	100	103	106	109	2
			114	117	94	98	90	101	104	107	110	3
		0	131	63	66	74	62‡, 71	77	80	83	134	1
			132	64	67	75	72	78	81	84	135	2
			133	65	68	76	73	79	82	87	136	3
		5	124	128	142	145	138,141‡	148	151	118	121	1
			125	129	143	146	139	149	152	119	122	2
			126	130	144	147	140	150	153	120	123	3
5.5		-5			194		198		201			1
					195		199		202			2
					196		200		203			3
		0		160	185		159‡		188	191		1
				182	186		157+		189	192		2
				184	187		158+		190	193		3
		5			204		207		210			1
					205		208		211			2
					206		209		212			3
	5.0	0		167	171		165+, 166‡		175	178		1
				170	172		163		176	179		2
				169	174		164		177	181		3

NOTES:

No superscript - normal model attitude as defined by NASA/MMA matrix

\+ - Model rolled to show cable tray
$\alpha_s = 0$, roll model = -31.5 deg

‡ - Model inverted to show cable tray on bottom of tunnel or get inverted data

—— Boundary layer trips on Model. Groups 9, 10, 11 used two twisted 4 mil wires. Groups 55, 56, 57 used #60 grit.

No data on groups 1, 58, 86, 95, 137, 154, 155, 161, 197, 213, 254, 309 - zero grou

Invalid data on groups 18, 54, 59, 60, 61, 69, 70, 85, 86, 108, 127, 156, 162, 168, 173, 180, 183

All invalid data groups were repeated.

TABLE 2. TEST DATA SUMMARY

b. Protuberances Off Model

M_∞	$Re_\infty \times 10^{-6}$ ft^{-1}	α, deg	β, deg. ←						→			Sw. Pos.
			-11	-9	-6	-3	0	3	6	9	11	
3.0	3.7	-5			325	328	331	334	337			1
					326	329	332	335	338			2
		↓			327	330	333	336	339			3
		0			313	316	310+	319	322			1
					314	317	311+	320	323			2
		↓			315	318	312+	321	324			3
		5										1
												2
		↓										3
4.0		-5	300	303	282	285	306	288	291	294	297	1
			301	304	283	286	307	289	292	295	298	2
		↓	302	305	284	287	308	290	293	296	299	3
		0	258	273	276	279	255+	264	267	270	261	1
			259	274	277	280	256+	265	268	271	262	2
		↓	260	275	278	281	257+	266	269	272	263	3
		5										1
												2
		↓										3
5.5		-5			229		232		235			1
					230		233		236			2
		↓			231		234		237			3
		0		217	220		214+		223	226		1
				218	221		215+		224	227		2
		↓		219	222		216+		225	228		3
		5										1
												2
		↓										3
	5.0	0		241	244		238+		247,253	250		1
				242	245		239+		248	251		2
	↓	↓		243	246		240+		249	252		3

NOTES:

No superscript - normal model attitude as defined by NASA/MMA matrix

+ - Model rolled to show cable tray
$\alpha_s = 0$, roll model = -31.5 deg

‡ - Model inverted to show cable tray on bottom of tunnel or get inverted data

—— Boundary layer trips on model. Groups 9,10,11 used two twisted 4 mil wires. Groups 55,56,57 used #60 grit.